Dai *et al. Soft Sci* 2023;3:7
DOI: 10.20517/ss.2022.30

Soft Science

Review Article

Open Access

Organic biodegradable piezoelectric materials and their potential applications as bioelectronics

Fanqi Dai[1], Qifan Geng[2], Tingyu Hua[2], Xing Sheng[3], Lan Yin[1,*]

[1]School of Materials Science and Engineering, The Key Laboratory of Advanced Materials of Ministry of Education, State Key Laboratory of New Ceramics and Fine Processing, Center for Flexible Electronics Technology, Tsinghua University, Beijing 100084, China.
[2]Weiyang College, Tsinghua University, Beijing 100084, China.
[3]Department of Electronic Engineering, Beijing National Research Center for Information Science and Technology, Institute for Precision Medicine, Center for Flexible Electronics Technology, and IDG/McGovern Institute for Brain Research, Tsinghua University, Beijing 100084, China.

***Correspondence to:** Prof. Lan Yin, School of Materials Science and Engineering, Yi-Fu Building of Science and Technology, Tsinghua University, Beijing 100084, China. E-mail: lanyin@tsinghua.edu.cn

How to cite this article: Dai F, Geng Q, Hua T, Sheng X, Yin L. Organic biodegradable piezoelectric materials and their potential applications as bioelectronics. *Soft Sci* 2023;3:7. https://dx.doi.org/10.20517/ss.2022.30

Received: 30 Nov 2022 **First Decision:** 5 Jan 2023 **Revised:** 19 Jan 2023 **Accepted:** 7 Feb 2023 **Published:** 24 Feb 2023

Academic Editor: Chuan Fei Guo **Copy Editor:** Fangling Lan **Production Editor:** Fangling Lan

Abstract

Biodegradable piezoelectrics represent an intriguing category of electroactive materials combining the mechanical-electrical coupling characteristics with a unique biodegradable feature that eliminates unnecessary materials retention and minimize associated infection risks. Here, we review the piezoelectric properties of representative organic biodegradable piezoelectric materials including amino acids, peptides, proteins, synthetic polymers and polysaccharides. Strategies to promote the piezoelectric activity are summarized, and recent progress in the utilization of biodegradable piezoelectric materials for bioelectronics is discussed, with perspectives and challenges provided at the end to enlighten possible future directions.

Keywords: Organic piezoelectric materials, biodegradation, bioelectronics

INTRODUCTION

Piezoelectrics represent a category of materials that generate electrical charges in response to mechanical stress and vice versa, and have been extensively explored for power devices, transducers, pressure sensors, *etc.*[1,2]. Although conventional piezoelectric materials such as zinc oxide (ZnO)[3], lead zirconate

titanate ($Pb(Zr_xTi_{1-x})O_3$, PZT)[4,5], barium titanate ($BaTiO_3$, BTO)[6-8], lithium niobate ($LiNbO_3$, LN)[9], potassium sodium niobate ($(K, Na)NbO_3$, KNN)[10], polyvinylidene fluoride (PVDF) and its copolymers[11-13] have demonstrated excellent piezoelectric properties, the presence of toxic or non-biodegradable constituents poses great challenges for use as biomedical implants. Although biotoxicity could be controlled by encapsulation, potential leakage of hazardous constituents still exists, and the non-degradable components could result in unnecessary materials retention associated with infection risks and dilemma of materials retraction. By contrast, biodegradable organic piezoelectric materials are attracting great interest due to their desirable biocompatibility and biodegradability that could eliminate retrieval surgeries[14-16]. Materials candidates include synthetic biodegradable polymers (e.g., poly(L-lactic acid), PLLA), protein-based polymers (e.g., gelatin), polysaccharides (e.g., chitosan) and amino acids. Although the piezoelectric constants of organic biodegradable materials are often much smaller compared with non-degradable piezoelectric materials, various strategies have been proposed which could greatly promote piezoelectric response by orders of magnitude [Figure 1], enabling practical therapeutic or diagnostic functions for biomedicine.

In this paper, we will first review the properties of representative organic biodegradable piezoelectric materials, followed by a discussion of fabrication strategies to achieve enhanced piezoelectricity. Recently demonstrated applications associated with organic biodegradable piezoelectric materials will be summarized, and challenges and future perspectives will be given at the end.

BIODEGRADABLE ORGANIC PIEZOELECTRIC MATERIALS

The piezoelectricity of small biomolecules such as amino acids or dipeptides originates from non-centrosymmetry. The hierarchical structure, such as folding and hydrogen bond (HB) network of large molecules, also plays a critical role in piezoelectric activity. The piezoelectric constants of representative biodegradable organic piezoelectric materials are summarized in Figure 1. Depending on the measurement, piezoelectric coefficients are reported in pC/N (based on the positive piezoelectric effect) or pm/V (based on the inverse piezoelectric effect). The associated piezoelectric properties will be discussed in the following sessions in terms of piezoelectric small molecules, piezoelectric materials with higher-order structure and piezoelectrets.

Piezoelectric properties of small biomolecules with non-centrosymmetric structure

Small biomolecules, such as some types of amino acids and dipeptides that have non-centrosymmetric structure, will give rise to net polarization and therefore piezoelectricity. As shown in Figure 2A, amino acids consist of an amino group ($-NH_2$), a carboxyl group (-COOH), and a side chain group (R group). Early works by Lemanov *et al.* showed over 16 amino acids and their compounds are piezoelectric, with glycine and DL-alanine exhibiting the best piezoelectric properties[17,18]. In ambient conditions, glycine has three polymorphic forms[19], including alfa (α), beta (β) and gamma (γ) glycine. α-glycine has a centrosymmetric structure that does not endow piezoelectricity, whereas β-glycine and γ-glycine have non-centrosymmetry, which results in net polarization, as illustrated in Figure 2B[20]. Guerin *et al.* calculated the theoretical values of piezoelectric effects of glycine in different polymorphic phases through density functional theory (DFT), which matched well with experimentally measured results (d_{16} = 178 ± 11 pm/V, d_{22} = 4.7 pm/V for β-glycine, and d_{11} = 1.7 pm/V, d_{22} = -1.1 pm/V, d_{33} = 9.93 pm/V for γ-glycine)[21]. The interestingly high shear piezoelectric constant (d_{16}) of β-glycine was attributed to molecular packing, elasticity and permittivity of the materials. Nevertheless, β-glycine is thermodynamically unstable, and strategies such as crystal growth of β-glycine in micro/nano-scale[22,23] and composites with polymeric nanofibers[24] or films such as chitosan[25], and mixture of different polymorphic glycine[25] were reported to address the issue. Recently, Yang *et al.* achieved wafer-scale bio-organic films consisting of crystalline

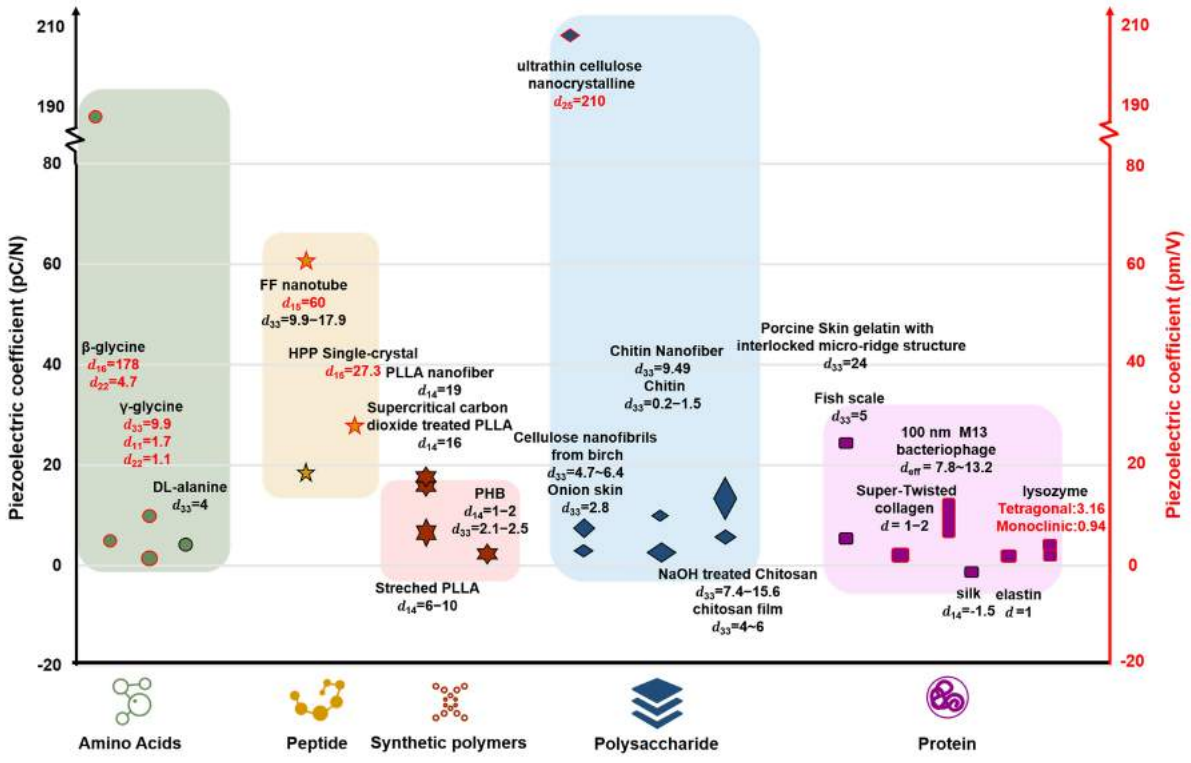

Figure 1. Piezoelectric constants of organic biodegradable piezoelectric materials. Symbols with a black border and reported values in black indicate piezoelectric coefficient in pC/N, and symbols with a red border and reported values in red indicate piezoelectric coefficient in pm/V.

γ-glycine layer sandwiched between polyvinyl alcohol (PVA) through HB guided self-alignment, with a maximum piezoelectric constant of 5.7 pC/N (d_{33})[26].

DL-alanine crystal has an orthogonal structure composed of two kinds of optical-active alanine molecules. In contrast to L-alanine, where the dipoles cancel each other out within the crystal, there is an alternating parallel layer between the L and D isomers within the racemic DL-alanine, resulting in a strong net polarization in the unit cell[27]. The average d_{33} of DL-alanine crystal is about 4 pC/N. Figure 2C illustrates the difference in crystal structure between L-alanine and DL-alanine. It is worth mentioning that piezoelectric amino acid crystals usually have low dielectric constant (ε) values together with modest piezoelectric strain constant (d_{ij}) values, which results in high piezoelectric voltage constant ($g_{ij} = d_{ij}/\varepsilon$) values with voltage outputs equivalent to those of inorganic ceramics[21,27]. The highest reported piezoelectric voltage constants of γ-glycine[21], β-glycine[21] and DL-alanine[27] are 0.46 V·m·N^{-1}, 8.13 V·m·N^{-1}, 0.82 V·m·N^{-1}, respectively, which are higher than those of PZT[28] (0.25 V·m·N^{-1}). These characteristics offer an important foundation for applications in bioelectronic devices.

Peptides are short chains of amino acids linked by peptide bonds and strong piezoelectric effects have also been observed in some peptide crystals due to their non-centrosymmetric structure. Diphenylalanine (FF), a peptide found in amyloid in Alzheimer's disease[29,30], is a representative small molecule peptide with intriguing piezoelectric properties[31-33]. FF molecules can be self-assembled into various nano/microstructures in solutions through electrostatic forces, solvent-mediated force, -stacking or hydrogen bonding[34]. All-atom explicit solvent MD simulation has been performed to demonstrate that the driving force of FF nanotube formation was step dependent, in the sense that electrostatics was dominant

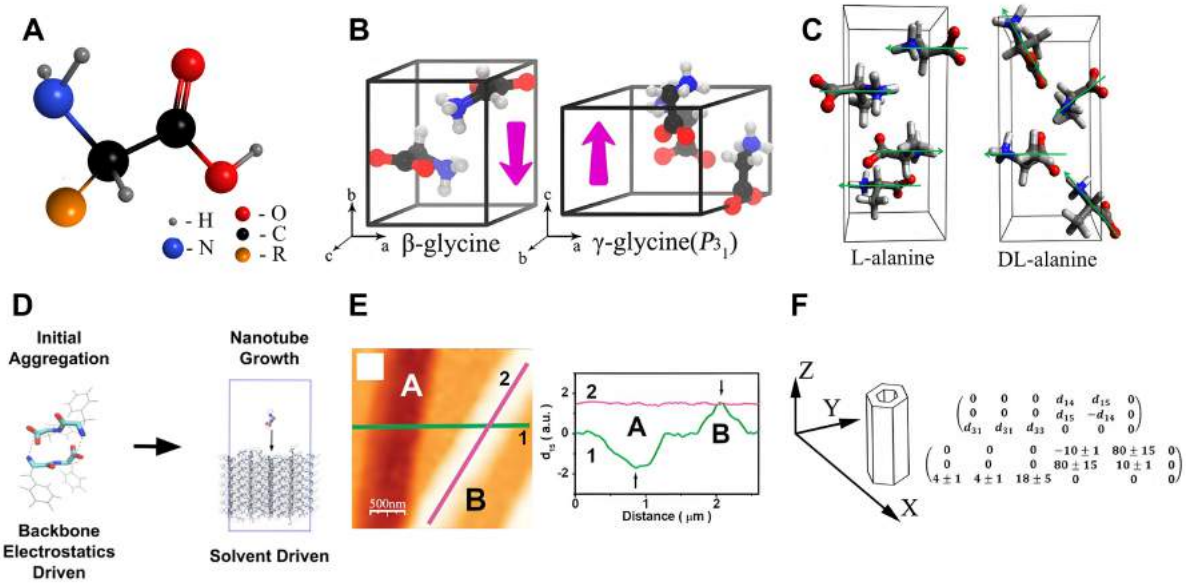

Figure 2. Piezoelectric properties of small biomolecules with non-centrosymmetric structure. (A) Schematic illustration of an amino acid molecule. (B) Crystal structure and molecular dipoles of β- glycine and γ-glycine. Reproduced with permission[20]. Copyright 2019, American Chemical Society. (C) Crystal structure of L-alanine and DL-alanine, and the latter has a stronger net polarization. Reproduced with permission[27]. Copyright 2019, American Physical Society. (D) Molecular dynamic (MD) simulation of the step-dependent driving force of diphenylalanine (FF) peptide nanotubes. Reproduced with permission[35]. Copyright 2018, American Chemical Society. (E) In-plane (IP) signal of two FF peptide nanotubes (A and B) with opposite polarizations demonstrate a strong d15 shear piezoelectric response. Reproduced with permission[31]. Copyright 2010, American Chemical Society. (F) Entire matrix of piezoelectric constants of FF peptide nanotubes obtained from the solution. piezoelectric response. Reproduced with permission[33]. Copyright 2016, Elsevier.

initially and the solvent-mediated force played an important role in subsequent growth of nanotubes [Figure 2D][35]. Kholkin *et al.* characterized the shear piezoelectric properties of a single FF nanotube through piezoresponse force microscopy (PFM), as shown in Figure 2E[31]. The work showed that the electric polarization of FF peptide nanotubes (PNTs) was along the tube axis, and the shear piezoelectric constant d_{15} was measured to be over 60 pm/V for nanotubes with a diameter around 200 nm, which was close to the inorganic piezoelectric ceramics lithium niobate ($LiNbO_3$, LN). Nguyen *et al.* demonstrated that the piezoelectric constant d_{33} of vertically aligned polarized FF nanotubes was approximately 9.9 pm/V, and can be promoted to a maximum of 17.9 pm/V by an electric field polarization process applied during the self-assembly growth of the peptide[36,37]. Vasilev *et al.* characterized the integral matrix of the piezoelectric constants of FF nanotubes grown from solutions, as shown in Figure 2F[33]. The relationship between d_{15} value and temperature was also assessed, and the results showed that piezoelectric response irreversibly decreased from approximately 50 pm/V to 32-35 pm/V when heated to 120 °C.

Piezoelectric properties of organic molecules with higher-order structure

The piezoelectric characteristics of macromolecules like long-chain peptides, proteins, polysaccharides and synthetic polymers are determined not only by intramolecular dipoles, but also hierarchical structures, such as HB networks, spatial folding, helical and fibrous structures[38]. Interestingly, Bera *et al.* demonstrated that even a tripeptide (Hydroxyproline-Phenylalanine-Phenylalanine, Hyp-Phe-Phe) can be engineered to achieve a helical structure mimicking the collagen structure through HB and aromatic zipper-like packing, as shown in Figure 3A[39]. The piezoelectric constant of the helical Hyp-Phe-Phe peptide (d_{16} = 27.3 pm/V) was much greater than that of β-folded tripeptides.

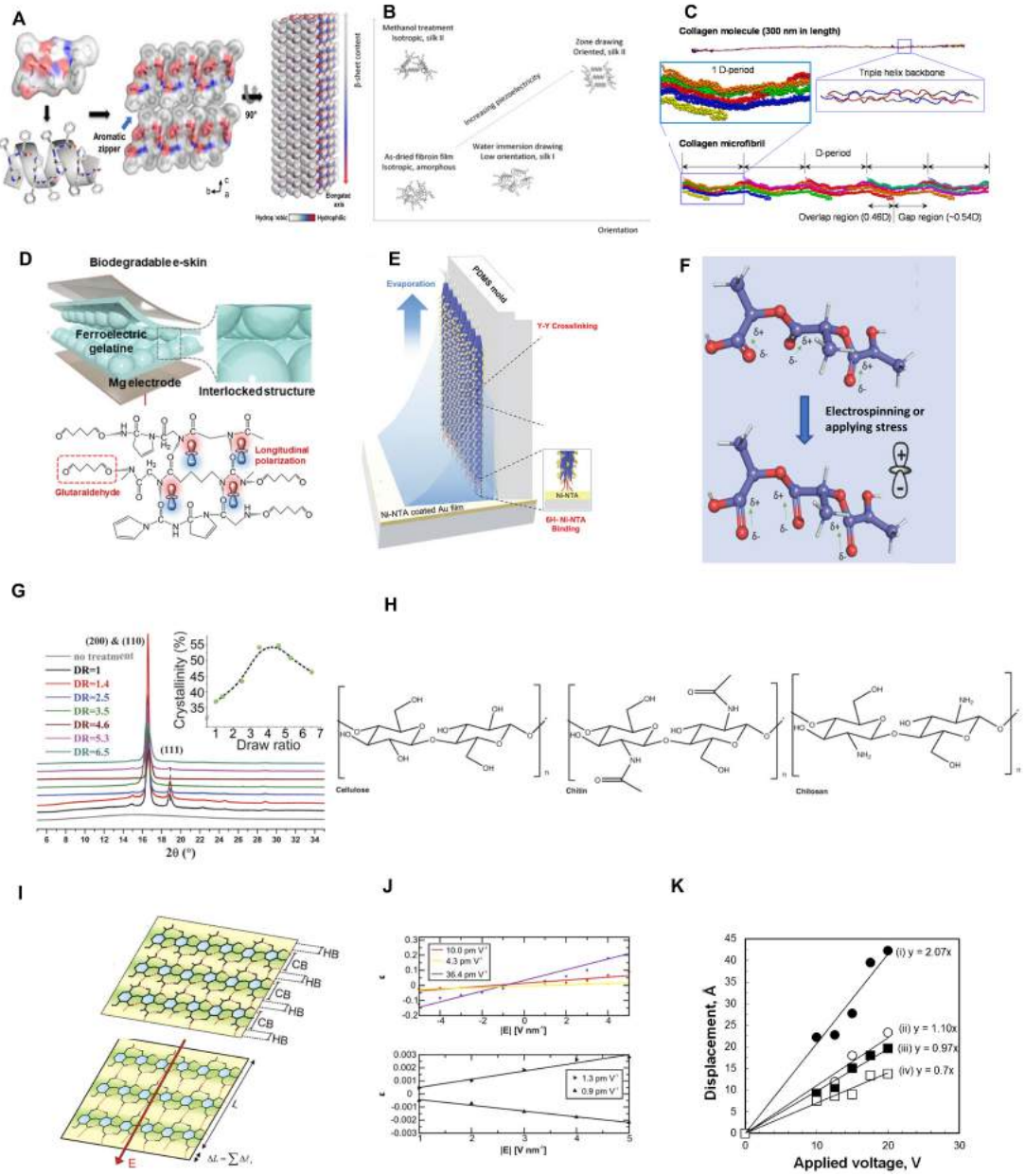

Figure 3. Piezoelectric properties of organic molecules with higher-order structure. (A) Hydroxyproline-Phenylalanine-Phenylalanine (Hyp-Phe-Phe) single-crystals are attracted through intermolecular hydrogen bonds (HB) and aromatic zipper-like packing, and form a helical stacking structure. Reproduced with permission[39]. Copyright 2021, Springer Nature. (B) The β-sheet content and crystal orientation determine the piezoelectricity of silk fibroin. Reproduced with permission[40]. Copyright 2011, John Wiley and Sons. (C) Atomic models of a single collagen molecule and collagen microfibril with five D-periods (each D period of around 67 nm). Reproduced with permission[41]. Copyright 2016, American Chemical Society. (D) Schematic illustration of the interlocked structure of the gelatin film cross-linked by glutaraldehyde with microdome structure. Reproduced with permission[49]. Copyright 2021, John Wiley and Sons. (E) Schematic illustration of the vertically polarized M13 bacteriophage nanostructure filled in polydimethylsiloxane (PDMS) microfluidic channels. Reproduced with permission[54]. Copyright 2019, American Chemical Society. (F) Dipoles on the poly(L-lactic acid) (PLLA) molecular chain are oriented to the same direction after stretching. Reproduced with permission[1]. Copyright 2019, John Wiley and Sons. (G) Dipoles on the PLLA molecular chain are oriented to the same direction after applying stress. Reproduced with permission[67]. Copyright 2018, National Academy of Science. (H) Chemical structure of cellulose, chitosan and chitin. Reproduced with permission[38]. Copyright 2021, Elsevier. (I) Schematic illustration of covalent bonds (CB) and HB arrangements in 2D nanocellulose crystal. (J) Calculated piezoelectric responses for single HB (upper) and extended crystal (lower). (K and I) reproduced with permission[80]. Copyright 2016, Springer Nature. (K) Vertical displacement of cellulose nanocrystal thin films with different alignment corresponding to externally applied electric fields. Reproduced with permission[82]. Copyright 2012, American Chemical Society.

Proteins are large molecules consisting of amino acids linked by peptide bonds. Many kinds of proteins, including silk, collagen, elastin and lysozyme, demonstrate different levels of piezoelectric properties depending on the chemistry and structure. Figure 3B demonstrates the relationship between the macroscopic piezoelectric properties of silk fibroin, the β-sheet content and the degree of orientation, which indicates crystallinity and crystal orientation are critical for enhancing piezoelectricity[40]. Stretched silk films can have a piezoelectric constant of up to 1.5 pC/N (d_{14}). With all-atom simulation [Figure 3C], Zhou *et al.* showed that the piezoelectric properties (1-2 pm/V) of collagen come from the polar and charged groups of collagen molecules, and the orientation and magnitude of the permanent dipoles changes along the long axis of the fibril under mechanical stress, which results in piezoelectricity[41]. Ghosh *et al.* reported a piezoelectric constant of about 5 pC/N (d_{33}) in demineralized fish scale layers (composed of self-assembled and ordered collagen nanofibrils)[42]. Elastin is a protein found in all connective tissues, especially elastic tissues such as tendons and arteries[43]. Liu *et al.* measured the piezoelectric effect of aortic elastin with the PFM technique and demonstrated a piezoelectric constant of about 1 pm/V[44]. In addition, the structure of an elastin monomer has a similar spontaneous polarization to classical perovskite-type cells, indicating the ferroelectric nature of elastin. Lysozyme is a globular protein in the secretions of egg white and mammals[45]. Stapleton *et al.* obtained tetragonal and aggregate films of monoclinic lysozyme and the average piezoelectric constants were measured to be 3.16 pC/N and 0.94 pC/N, respectively[46]. In general, the piezoelectric constants of protein macromolecules are weak[40,42,44,47,48] due to low crystallinity and complex dipole orientation. Nevertheless, appropriate structure design is beneficial to improve the piezoelectric properties. Ghosh *et al.* fabricated an interlocked microdome structure of pigskin gelatin cross-linked by glutaraldehyde (GA) to physically confine peptide chains [Figure 3D], which resulted in increased piezoelectricity[49]. The d_{33} value of the gelatin microdome film was about 24 pC/N, which is six times the piezoelectric constant of conventional gelatin.

The structure of viruses is more complex than the previously mentioned proteins and M13 bacteriophage represents an interesting virus that exhibits strong piezoelectric properties due to the presence of unique protein components[45]. M13 bacteriophage is covered by about 2700 copies of a major coat protein (PVIII) and five copies of minor coat proteins (PIII and PIX) located at either end[50-52]. The α-helix structure of the PVIII proteins results in a dipole moment directed from the amino-terminal to the carboxy-terminal. Lee *et al.* firstly observed both longitudinal and shear piezoelectric effects of M13 bacteriophage with the PFM technique[52]. Wild-type (WT)-phage monolayer films exhibited an effective piezoelectric coefficient (d_{eff}) value of 0.3 ± 0.03 pm/V. Recombinant DNA techniques allowed the engineering of charge distribution on the surface of PVIII by inserting negatively charged amino-acid glutamate (E) to modulate the overall dipole moment. The d_{eff} value of the 4E-phage (with two extra glutamates added) monolayer films reached a value of 0.7 ± 0.05 pm/V. Furthermore, the piezoelectric property of M13 bacteriophage could be further improved by controlling the thickness of the membrane. A WT-phage membrane(100 nm) exhibited a d_{33} value of 7.8 pm/V, and the piezoelectric coefficient of 4E-phage membrane could reach 13.2 pm/V. In addition, M13 bacteriophage can obtain vertically ordered unidirectional polarized structure with higher piezoelectric properties by tuning orientation, polarization direction, microstructure morphology and density. Shin *et al.* fabricated phage nanopillars (PNPs) by completely filling a porous anodic aluminum oxide (AAO) template with M13 bacteriophage, and achieved a nanogenerator wrapped with a polydimethylsiloxane (PDMS) elastomer layer, with a piezoelectric constant of 6.1 ± 0.1 pm/V[53]. Lee *et al.* infiltrated phage suspensions into PDMS molds with microfluidic channels [Figure 3E] and realized tyrosine(Y)-mediated cross-links between the phages by evaporating solvents through ultraviolet irradiation[54]. Hexa-histidine (6H) was also inserted into the N-terminal of PIII to polarize the binding of phages on the substrate. In addition, the dipole moment can be enhanced by fusing three glutamates (3E) at the N-terminal of PVIII, and the peak voltage and current of the piezoelectric energy harvester reached 2.8 V and 120 nA, respectively. In general, M13 bacteriophage has stronger piezoelectric properties than

most proteins, and can be genetically engineered to modulate their properties and produced in large quantities by means such as bacterial infection and mass-amplification[55]. Nevertheless, the piezoelectric mechanism at the molecular level of M13 bacteriophage is not well understood, and further investigations are still needed[2].

Piezoelectric synthetic polymers follow a similar piezoelectric mechanism. One of the most prevalent biodegradable piezoelectric polymers is poly(L-lactic acid) (PLLA). PLLA has three different crystalline modifications (α, β, γ)[56]. The most common phase of PLLA is α-phase, which presents a 10_3-helix conformation and pseudo-orthorhombic units[56,57]. The β-phase, which has a 3_1-helix conformation, can be produced under stretching and annealing conditions[58]. The γ-phase, which is metastable and can be easily converted to α-phase over heating[59], could be grown epitaxially on hexamethylbenzene (HMB) crystalline substrate[60]. Researchers have revealed that the point group of PLLA crystal is D_∞-∞22, which results in two independent shear piezoelectric constants, d_{14} and d_{25}[61]. The C=O dipoles of α-phase and β-phase are oriented along the main chain of PLLA, and the application of shear stress rotates the C=O dipoles in the helical backbone, resulting in the alignment of dipole moments and therefore shear piezoelectricity[62]. PLLA is often processed into films that consist of crystal (piezoelectric phase) and amorphous (non-piezoelectric phase) regions[63]. Lovell *et al.* demonstrated the linear relationship between the shear piezoelectric effect of PLLA films and the crystallinity index and orientation coefficient[64]. Untreated PLLA films usually have very weak macroscopic piezoelectricity due to their complex higher-order structure of amorphous domain that induces low translational symmetry[65]. The introduction of processing such as uniaxial stretching[66,67], electrical polarization[68] and electrospinning process[69-72] can align dipoles on PLLA molecular chains and greatly promote the crystallinity and piezoelectric properties, as shown in Figure 3F[1]. For example, Curry *et al.* showed that the crystallinity of PLLA films changed as a function of stretching ratio and reached a peak value around 4-5 fold of stretching [Figure 3G], and d_{14} of uniaxially stretched PLLA films realized a value of 6-10 pC/N[66,67]. The highly oriented PLLA nanofibers obtained by electrospinning progress can reach a higher piezoelectric coefficient of 19 pC/N[72]. Supercritical carbon dioxide (sc-CO_2) treatment[73,74] has also been demonstrated to improve the macroscopic piezoelectric properties of PLLA with a d_{14} value of 16pC/N, by partially removing the amorphous component and enhancing crystallinity. In addition, biodegradable polymer polyhydroxybutyrate (PHB)[75] also possess piezoelectricity after stretching or electrospinning (d_{14} = 1-2 pC/N, d_{33} = 2.1-2.5 pC/N)[76-78]. To improve the mechanical properties of PHB for *in vivo* applications, composites with other polymers such as poly(ε-caprolactone) (PCL) have been proposed[79].

Polysaccharides are long-chain polymeric carbohydrates made of a number of monosaccharide units. Some polysaccharides, such as cellulose, chitosan and chitin, exhibit relatively strong piezoelectric effects due to their special low-symmetry fiber structure[2]. The molecular structure of these polysaccharides appears in Figure 3H[38]. Garcia *et al.*[80] predicted the in-layer piezoelectricity of Iβ-cellulose (the stable crystalline phase of cellulose[81]) in the 2D nanocrystal format consisting of covalent bonds (CB) and HB [Figure 3I], and suggested that the piezoelectricity originated from the HB network. The calculated piezoelectric constant of individual HB ranged from 4.3 to 36.4 pm/V, while the overall piezoelectric constants of the extended crystal were predicted to be 1.3 pm/V(d_{22}) and 0.9 pm/V (d_{11}), as shown in Figure 3J. Csoka *et al.* have also reported a large shear piezoelectric constant of ultrathin films of highly aligned cellulose nanocrystals to be around 210 pm/V (d_{25}) by PFM measurement [Figure 3K], which was ascribed to the chain arrangement and dipole moments in the crystalline cellulose[82]. The cellulose layers of plants in nature also demonstrated weak piezoelectric properties constant due to the presence of large portions of amorphous components and opposite dipoles. For instance, onion skins exhibited a d_{33} value of about 2.8 pC/N[83], and cellulose nanofibrils extracted from birch reached a d_{33} value of 4.7-6.4 pC/N[84]. Moreover, chitosan showed

piezoelectricity around 4-6 pC/N and was mostly used as a biocompatible matrix to achieve piezoelectric composites[25,85]. Recent work by Marzo *et al.* has accomplished significantly improved piezoelectricity of chitosan (7.4~15.6 pC/N) through neutralizing treatment with NaOH solutions by promoting the crystallinity[86]. Similarly, although the piezoelectric constants of chitin are mostly between 0.2~1.5 pC/N[87], Hoque *et al.* reported chitin nanofibers extracted from crab shells with piezoelectric constants as high as 9.49 pC/N (d_{33})[88].

Piezoelectrets

Polymer films with cellular structure showed strong piezoelectric activity after proper poling, and these electroactive materials are referred to as piezoelectrets. Zhukov *et al.* reported a biodegradable polylactic acid (PLA) piezoelectret by corona polarization and the piezoelectric constant d_{33} can reach a maximum value of 600 pC/N, as shown in Figure 4A[89]. Although the piezoelectric effect was reduced by half compared with the initial value in the first 20 days after polarization, it remained stable for the next 130 days. Gao *et al.* constructed a biodegradable paper-based electret nanogenerator using transparent cellulose nanopaper (t-paper) and PLA piezoelectret layer, as shown in Figure 4B[90]. The comparison of output current with and without PLA piezo-electret layer under periodic pressing indicated that the mechanical-electrical response was attributed to the PLA piezo-electret layer which can be strongly polarized and reliably maintain the charges [Figure 4C]. The piezoelectric effect of piezo-electrets is mostly affected by the cellular structure (cell density, shape and size), relative density and elastic stiffness, electrical breakdown strength, service temperature, *etc.*[91,92]. Piezoelectrets provide an alternative way to achieve biodegradable devices with desirable piezoelectricity that can adapt to versatile biomedical applications. Nevertheless, further studies are needed to verify the long-term stability of piezoelectrets in humid environments, which is essential for biological applications.

Biodegradation of piezoelectric materials

The aforementioned materials not only demonstrate piezoelectricity activity relevant for bioelectronics, but also possesses biodegradability that can avoid unnecessary materials retention in biological systems. Amino acids, peptides or proteins play an important role in a number of biological processes. Peptides and proteins can breakdown into amino acids, which will be metabolized by transamination to ammonia[93]. Studies have shown that M13 bacteriophage has good biodegradability in different body fluids and tissues (blood, urine, saliva, artificial gastric juice (AGJ), and mouse homogenates of stomach, jejunum, and colon, *etc.*)[94]. The highest degradation rate (nearly 100% after 45 mins) was found in jejunum homogenate, which was rich in proteolytic enzymes. Regarding biosafety, M13 bacteriophage possesses a specific tropism to interact with host bacterial cells and does not attack mammalian cells[50,95,96]. Synthetic biodegradable polymers have already been widely used in biomedicine. For example, PLLA has been approved by US Food and Drug Administration (FDA) as implants and has been adopted as biodegradable sutures and cardiovascular stents. PLLA degrades through hydrolysis to lactic acid, and the final metabolite is water and carbon dioxide[97]. A significant decrease in molecular weight and mass was observed in the first 3 months after the subcutaneous implantation of PLLA samples in the rats[98], and complete breakdown occurred in a time frame of at least 4 years[97,99]. In addition, polysaccharides such as chitosan and chitin can be readily hydrolyzed by lysozyme, which is commonly found in mammals, while cellulose can only be hydrolyzed by microbial and fungal enzymes[100], which constrains its potential *in vivo* applications[101].

FABRICATION STRATEGIES FOR ENHANCED PIEZOELECTRICITY

Directional stretching, electrospinning, electrical poling and HB guided self-assembly are representative strategies that promote crystallinity and dipole alignment of biodegradable piezoelectric materials and achieve enhanced piezoelectric activity. Directional stretching induces alignment of dipoles in the microcrystalline and amorphous regions and promotes piezoelectricity [Figure 5A]. For example, PLLA

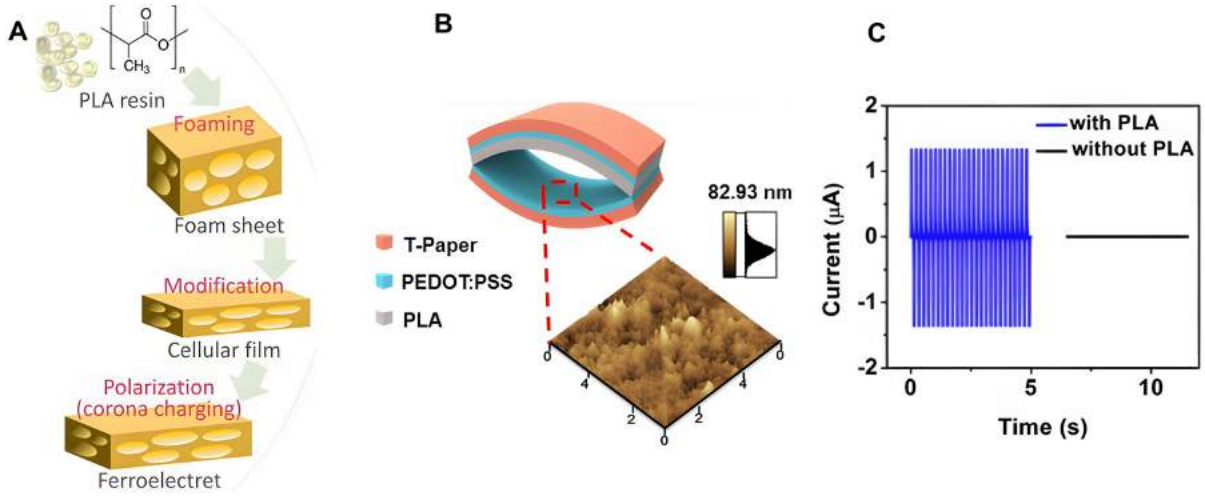

Figure 4. Piezoelectrets. (A) Fabrication process of the polylactic acid (PLA) piezoelectret. Reproduced with permission[89]. Copyright 2020, AIP Publishing LLC. (B) Device structure of a biodegradable and transparent paper-based electret nanogenerator constructed by a transparent cellulose nanopaper (Tpaper) and a PLA piezo-electret. (C) Piezoelectric output currents of the nanogenerator with and without the PLA electret. (B and C) reproduced with permission[90]. Copyright 2016, American Chemical Society.

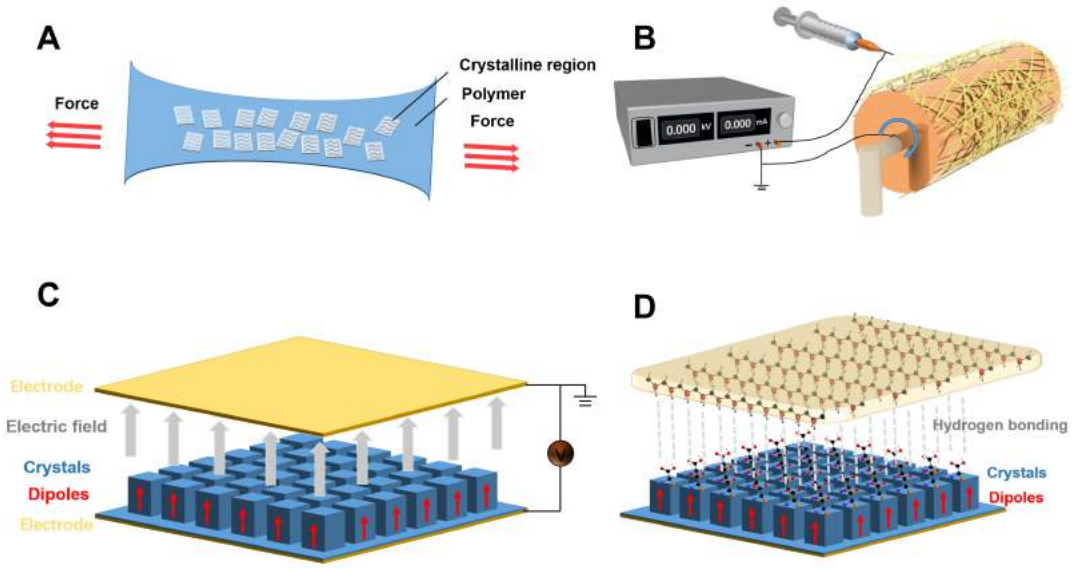

Figure 5. Strategies to enhance the piezoelectric properties of biodegradable materials. (A) Dipole alignment under tensile stress. (B) Schematic illustration of electrospinning. (C) Schematic illustration of the enhanced alignment of dipoles in the piezoelectric crystals under external applied electric field. (D) Schematic illustration of the enhanced alignment of dipoles induced by HB.

films processed with a stretching ratio of 4-5 greatly enhanced the crystallinity and boosted piezoelectric constant[67]. Electrospinning is another common process to enhance the properties of piezoelectric polymers [Figure 5B]. Studies have demonstrated that the electric field in the process of electrospinning can promote the orientation of a large number of dipoles toward the fiber direction or vertical direction[69,70], which enhanced piezoelectric properties[72]. Different mechanical properties and fiber orientation can be obtained by adjusting the processing parameters such as solution properties, electrical field strength and rotating speed of the receiving drum. For instance, as drum speeds increased from 1000 to 4000 rpm, the piezoelectric constant (d_{14}) value of the collected nanofibers increased from 9 pC/N to 19 pC/N, while the

nanofibers collected at 300 rpm drum speed show almost no piezoelectric properties[72]. Electrical poling during the growth of piezoelectric crystals can also assist the alignment of dipoles along the direction, which is beneficial to promote piezoelectricity [Figure 5C]. For instance, applying positive or negative electric field to the growth of FF nanotubes significantly improved the piezoelectric constants from 9.3 pm/V (no electric field) to 17.9 pm/V (negative electric field) or 11.7 pm/V (negative electric field)[37]. Moreover, intermolecular force (e.g., HB) plays an important role in promoting the orientation of dipole moments during the course of piezoelectric crystal growth, as shown in Figure 5D. Yang *et al.* utilized the HB at the PVA and γ-glycine interface to promote the self-assembling of glycine and accomplished a wafer-scale composite film with high piezoelectric response, flexibility and biodegradability[26]. The maximum d_{33} piezoelectric constant of the composite film was 5.7 pC/N, which was comparable to that of commercial PVDF piezoelectric films.

APPLICATIONS OF BIODEGRADABLE PIEZOELECTRIC MATERIALS FOR BIOELECTRONICS

Piezoelectric materials enable the conversion of external mechanical stimuli into electrical energy and vice versa and are prevalently used in sensors and energy harvesting[102]. In addition, the charges generated on the surface of piezoelectric materials can potentially be utilized as electronic medicine to regulate the behavior of cells and tissues[103]. Biodegradable piezoelectric materials have the advantage of natural degradation after operational windows, and can potentially eliminate material retention and associated infection risks.

Energy harvesting

Biodegradable piezoelectric materials have been explored as nanogenerators to convert mechanical movements to electrical energy. Given piezoelectric properties comparable to PVDF, FF peptides have been fabricated into piezoelectric nanogenerators (PENGs) with reliable performance[104,105]. Jenkins *et al.* showed that FF peptide nanowires can generate higher voltages than ZnO, PZT and BTO nanowires under the same force[104]. A flexible FF peptide nanogenerator was achieved, with an open-circuit voltage of 0.6 V and a short-circuit current of 7 nA under cyclic displacement. Lee *et al.* developed a meniscus-driven self-assembly process for the fabrication of horizontally aligned FF PNTs with large unidirectional polarization, as shown in Figure 6A[105]. The obtained nanogenerator was capable of providing an output up to 2.8 V, 37.4 nA, and 8.2 nW [Figure 6B]. Tao *et al.* designed and fabricated a flexible and biodegradable PENGs with FF PNTs and PLA was used to transfer FF peptide nanotubes from silicon substrates [Figure 6C][34]. The d_{33} value of the composite film was 12.4 pm/V, and the voltage and current output under different applied forces are shown in Figure 6D. The PENGs produced a power density of 1.56 W/m^3, which is higher than many reported PENGs based on biodegradable biomaterials. Zhao *et al.* reported a cantilever beam energy harvester based on double-layer heat-treated PLLA films, as shown in Figure 6E[106]. In this work, the PLLA films were subjected to thermal annealing (140 °C) for 5-24 h after tensile stretching (4-fold), and a high piezoelectric constant (d_{14}) of approximately 9.57 pC/N was obtained. The cantilever device can produce an output voltage of up to 9.4 V and a power output of 14.45 μW, which can charge a lithium battery and power multiple light-emitting diodes (LEDs) [Figure 6F]. In general, most biodegradable piezoelectric materials have strong shear piezoelectricity but weak transverse and longitudinal piezoelectric properties, thus often requiring customized structure to convert normal stress to in-plane shear stress, resulting in lower energy output than conventional energy-harvesting devices such as non-degradable piezoelectric nanogenerators[107], triboelectric nanogenerators[108], which could limit potential applications as power sources.

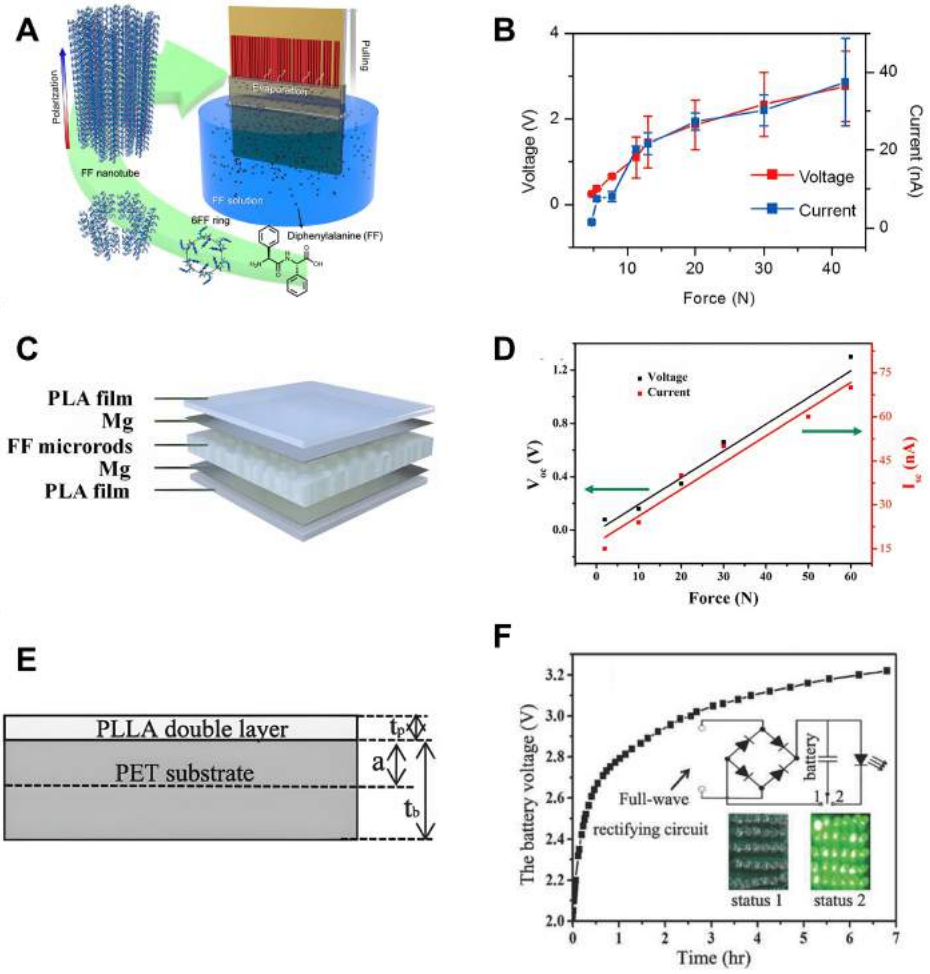

Figure 6. Energy harvesting. (A) Schematic illustration of the fabrication scheme to form large-scale aligned FF PNTs. (B) Output voltages and currents of FF PNT energy harvester as a function of applied force. (A and B) reproduced with permission[105]. Copyright 2018, American Chemical Society. (C) Schematic illustration of the structure of the biodegradable piezoelectric nanogenerators (PENGs) based on FF peptides enabled by PLA polymer-assisted transfer. (D) Voltage and current outputs of FF-based biodegradable PENGs under applied forces ranging from 2 to 60 N. c and d reproduced with permission[34]. Copyright 2021, Elsevier. (E) Schematic illustration of PLLA cantilever beam. (F) Voltagetime dependence of a lithium battery charged by the PLLA cantilever. The inset shows the charging circuit and the photograph of 30 LEDs lit by the battery. (E and F) reproduced with permission[106]. Copyright 2017, John Wiley and Sons.

Actuators, biosensors and transducers

The electromechanical conversion properties of piezoelectric materials allow the conversion of mechanical stimuli (pressure, bend, twist, *etc.*) into electrical signals, enabling real-time sensing (e.g., pressure and strain) in biological environments, which sets an important engineering basis for healthcare monitoring, smart devices and bionic prostheses[1,109]. Based on inverse piezoelectricity, piezoelectric materials also play a critical role as actuators and transducers when properly engineered, which is essential for applications such as controlled drug delivery and soft robotics[110].

Bioelectronics based on biodegradable piezoelectric materials have been developed for various actuators, sensors, and transducer systems[1,109,111]. For example, actuators made of piezoelectric PLLA have been realized as intelligent tweezers. Tajitsu *et al.* showed that PLLA fibers fabricated by dry jet spinning method produced significant vibration upon the application of AC voltage in the range of 50-300 V and the

frequency between 0.1-150 Hz, and could serve as electrically controlled conduits and micro tweezers[112]. The exfoliation of assumed thrombosis sample in blood vessels by the PLLA fiber catheter was demonstrated. Sawano *et al.* developed a sc-CO_2-treated PLLA, which had a larger piezoelectric constant, and achieved an electrical tweezer in a "Finger-joint-shaped" that was capable of performing complex movements such as grasping polystyrene beads [Figure 7A], which could achieve operations in constrained space such as small blood vessels[74].

Biodegradable piezoelectric materials with desirable flexibility that can produce large deformation under small forces are excellent candidates for building biodegradable sensors. Curry *et al.* proposed a biodegradable pressure sensor based on mechanically stretched PLLA film and demonstrated *in vivo* pressure monitoring in the abdominal diaphragm of mice, as shown in Figure 7B[67]. The sensor can accurately measure a wide pressure range (0-18 kPa) associated with physiological pressure, which could enable self-monitoring of vital signs such as intracranial pressure, intraocular pressure, intraarticular, *etc.* Hosseini *et al.* fabricated a flexible and biodegradable pressure sensor based on a composite film of β-glycine crystals and chitosan matrix with a sensitivity of 2.82 ± 0.2 $mV \cdot kPa^{-1}$[25]. The proposed device could be applied for wearable diagnostics and electrical stimulation for wound healing. Ghosh *et al.* fabricated a ferroelectric pigskin gelatin electronic skin (e-skin) [Figure 7C] with a microdome interlocked structure and achieved very high sensitivity (~41 $mV \cdot Pa^{-1}$) at low pressures with a detection limit near 0.005 Pa, even surpassing the non-biodegradable nanogenerators[49]. The device could sense the spatially resolved pressure and surface texture of an unknown object and be potentially deployed for pressure mapping and texture perception that are critical for healthcare monitoring. Liu *et al.* also reported a pressure sensor based on electrospun silk fibroin, as shown in Figure 7D[113]. The stress transferred from the electrode to the piezoelectric layer can be enhanced by surface-engineered electrodes fabricated by transfer printing using a metal mesh as the template, and the overall sensitivity of the device reached 30.6 mV/N, together with the advantages of fast response (3.4 ms), long cycle life (3000 cycles) and good linearity, which could be deployed for real-time detection such as oral cavity monitoring.

Transducers represent another category of devices for which biodegradable piezoelectric materials can be used. Kim *et al.* extracted β-chitin from squid and obtained a piezoelectric film with a piezoelectric constant of about 3.986 pm/V by centrifugal casting and hot pressing (120 °C)[114]. The flexible piezoelectric transducer worked well with paper-type speakers and microphones, and the synchronization rate with the original sound source was about 70%, providing a new route toward eco-friendly piezoelectric devices. Curry *et al.* proposed a highly oriented PLLA nanofiber film through electrospinning, which has been demonstrated for monitoring important physiological pressure *in vivo* and generating ultrasound to disrupt the blood-brain barrier (BBB), as shown in Figure 7E[72]. The biodegradable ultrasonic transducer can generate a sound pressure up to 0.3 MPa at a frequency of 1 MHz. The closer the coronary tissue of the mouse brain was to the implanted transducer, the more autofluorescent signals of blood protein (green stain, indicating leakage due to disrupted BBB) were detected [Figure 7F], whereas the blood protein was completely absent in the cases with non-piezoelectric films implanted, suggesting that the sound pressure generated by the biodegradable piezoelectric transducer can induce the opening of BBB. Moreover, piezoelectrets with large longitudinal piezoelectric constants serve as an alternative option to achieve biodegradable transducers. Dali *et al.* successfully fabricated a biodegradable ultrasonic transducer based on a PLA piezoelectret[115]. The transducer exhibited a large bandwidth of approximately 45 kHz and fractional bandwidth of 70%, resulting in sound pressure of 98 dB to 106 dB for driving voltages from 30 to 70 Vrms.

Therapeutics

Bioelectricity is essential in many physiological processes[116] and studies have explored electrical stimulation provided by biodegradable piezoelectric materials to assist the treatment of a variety of diseases, including

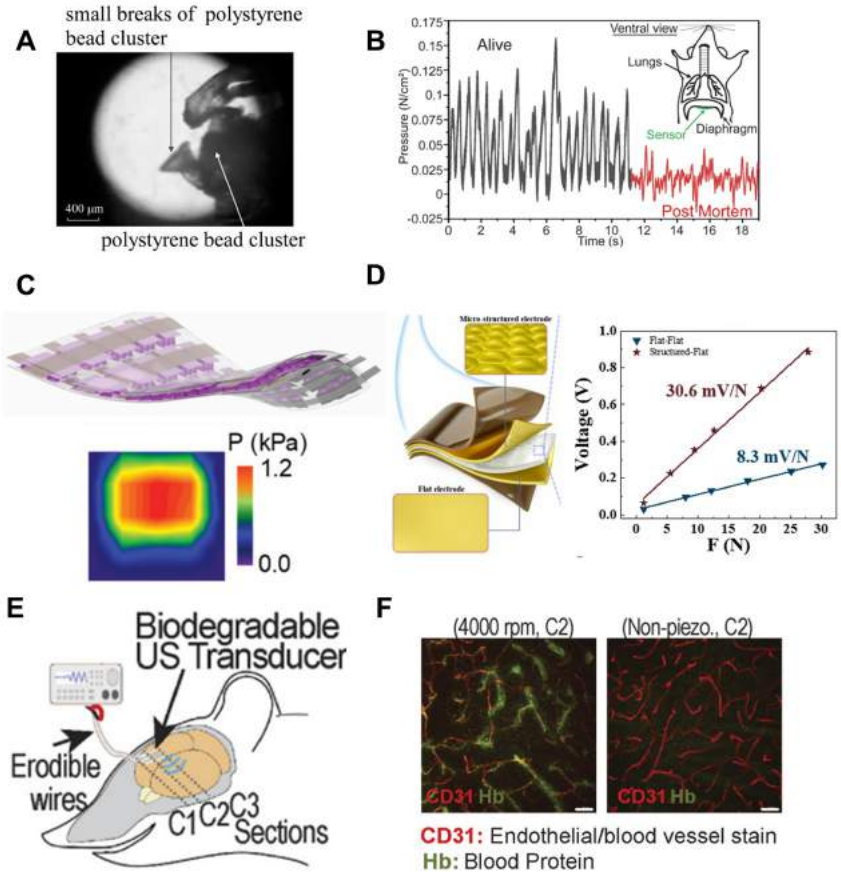

Figure 7. Actuators, biosensors and transducers based on biodegradable piezoelectric materials. (A) Optical Image of the grasping of a polystyrene bead cluster using PLLA actuator treated with supercritical-CO_2. Reproduced with permission[74]. Copyright 2010, John Wiley and Sons. (B) Pressure signals detected by the PLLA sensor in the mouse abdominal diaphragm, black line and red line represent live mouse under anesthesia and being euthanized, respectively. Reproduced with permission[67]. Copyright 2018, National Academy of Science. (C) Structure of the biodegradable ferroelectric gelatin electronic skin (e-skin) and the image of the pressure distribution when placed on an irregular object. Reproduced with permission[49]. Copyright 2021, John Wiley and Sons. (D) Schematic illustration of the structure of silk fibroin based pressure sensor with micro-structured electrode and the comparison of voltage response symbols and linear fits between silk sensor with micro-structured electrode and flat electrode. Reproduced with permission[113]. Copyright 2022, Elsevier. (E) Schematic illustration of the *in vivo* experiment of PLLA nanofiber transducer to overcome the blood-brain barrier. (F) The autofluorescent signal of blood protein (green stain) at the coronal section (C2) from the brains of mice that received ultrasound (US) from the piezoelectric PLLA transducer (left, 4000 rpm) and the non-piezoelectric PLLA transducer (right). (E and F) reproduced with permission[72]. Copyright 2020, National Academy of Science.

bone fractures, neurite growth, wound healing, *etc.*[117]. When a piezoelectric material is subjected to mechanical deformation, its internal dipoles are reoriented and piezoelectric charges are generated on the surface. The charges and associated electric field may trigger complex cell signaling pathways, such as opening calcium channels in cell membranes, resulting in an increase in the intracellular Ca^{2+} concentration to promote cell proliferation and differentiation[118]. In the case of cartilage and bone formation, the upregulation of the Ca^{2+} concentration can activate calmodulin, calcineurin and calcineurin dephosphorylates nuclear factor, which further translocate into the nucleus to elevate the expression of signaling proteins such as bone morphogenic proteins (BMPs) and growth factors such as TGF-β [Figure 8A][118]. Given similar piezoelectric activity as bone tissues[119], PLLA[120-122], PHB[123-125], collagen[126,127] and chitosan[128] based piezoelectric scaffolds have been developed as effective materials to promote the proliferation of bone cells or the repair of bone defects. Recently, Das *et al.* demonstrated the repair of the broken skulls of mice combining piezoelectric PLLA nanofiber scaffolds with ultrasound (US) treatments, as

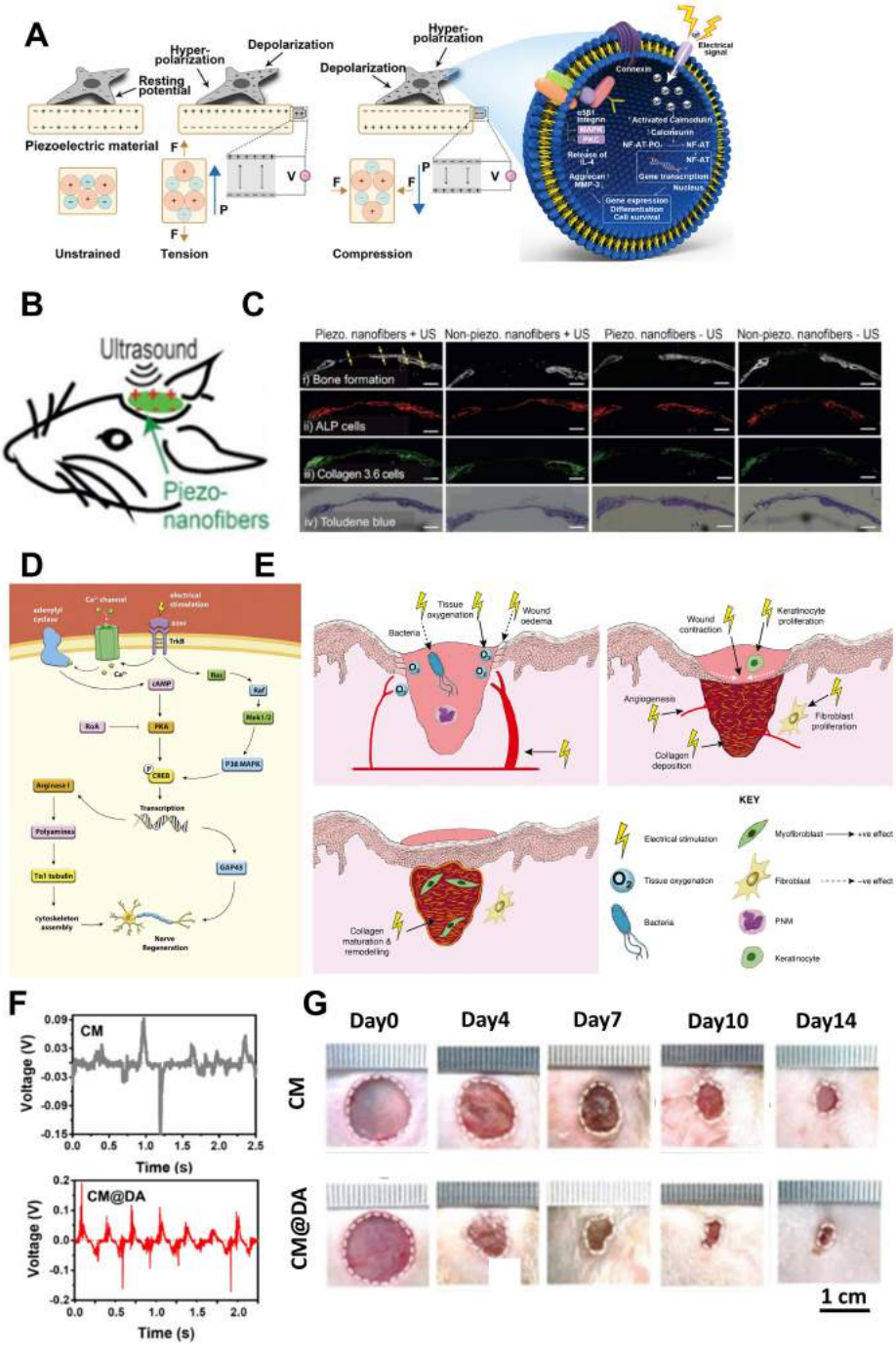

Figure 8. Therapeutic vehicles based on biodegradable piezoelectric materials. (A) Schematic illustration of surface charges generated by piezoelectric materials upon mechanical strain to trigger the signaling pathways of attached cells. Reproduced with permission[118]. Copyright 2020, John Wiley and sons. (B) Schematic illustration of the implantation of piezoelectric PLLA nanofiber covering the defects on the calvaria bone of mice. (C) Piezoelectric PLLA nanofiber with US effectively promote bone formation (yellow arrow) compared with the other groups. (B and C) reproduced with permission[129]. Copyright 2020, Elsevier. (D) Schematic illustration of electric field induced upregulation of regeneration-related genes in the neuronal cell body through calcium dependent mechanism. Reproduced with permission[134]. Copyright 2020, Elsevier. (E) Schematic illustration of three phases revealing the effects of electric fields on wound healing. Reproduced with permission[155]. Copyright 2016, John Wiley and sons. (F) *In vivo* output voltage curves of chitosan films (CM) and polydopamine coated chitosan films (CM@DA) immobilized on the back of mice. (G) Representative images of wounds on days 0, 4, 7, 10, and 14 after the treatment with CM and CM@DA films, respectively. (D and E) reproduced with permission[157]. Copyright 2020, Elsevier.

shown in Figure 8B[129]. *In vivo* experiment showed that the mice that received piezoelectric PLLA nanofiber films and US had much more new bone formation, and a greater amount of alkaline phosphatase (ALP) positive cells and green collagen 3.6 fluorescent signals (both represent higher osteogenic differentiation activity) than the ones from other groups with either no ultrasound or non-piezoelectric PLLA nanofibers [Figure 8C]. Liu *et al.* reported intriguing cartilage regeneration by the implantation of multi-layered PLLA nanofibers and collagen composites into the joints of rabbits[130]. The mechanical stimulation introduced by physical exercise can fully activate the piezoelectric scaffold, leading to complete healing of osteochondral defects in rabbits with abundant chondrocytes and type II collagen formation after 1-2 months.

In the case of peripheral nerve regeneration, studies have shown that the piezoelectric charges generated by piezoelectric materials could open the calcium channels of cell membranes and accelerate the influx of calcium ions from the extracellular fluid[131-133]. Associated brain-derived neurotrophic factor (BDNF) and tropomyosin kinase B (TrkB) in neuronal cell body could be consequently simulated and promote the expression of regeneration-related genes by upregulating cyclic adenosine monophosphate (cAMP) pathways, as shown in Figure 8D[134]. The induced electrical potential difference has also been shown to boost the proliferation of Schwann cells, the production of nerve growth factor (NGF) and remyelination on injured axons, which is beneficial in assisting nerve regeneration[135]. Composite materials consisting of biodegradable piezoelectric matrix and inorganic piezoelectric ceramic filler[136,137] capable of partial degradation have been proposed for nerve regeneration. Some fully biodegradable scaffolds developed based on the piezoelectric effect of biodegradable piezoelectric materials have also been investigated for neural regeneration. Ramakrishna *et al.* realized PLLA nanofiber scaffolds by phase separation and electrospinning that can promote the differentiation and growth of neural stem-like cells[138,139]. Chen *et al.* demonstrated the feasibility of poly(3-hydroxybutyrate-co-3-hydroxyvalerate) (PHBV) microspheres as a scaffold to support neuronal cell growth and axon-dendritic polarization[140]. Other bio-piezoelectric materials such as cellulose[141], chitin[142], chitosan[143,144], and collagen[145] have also been reported to be able to support cell adhesion and growth. Some of these materials have been made into nerve conduits for peripheral nerve regneration[146-150]. Jiang *et al.* constructed a novel chitosan-based nerve graft comprising microporous chitin-based conduit and internal carboxymethyl chitosan fiber and applied it to bridge sciatic nerve across a 10-mm defect in Sprague Dawley (SD) rats[150]. The artificial composite nerve graft could effectively promote the restoration of damaged neurons with similar efficacy compared to the autograft. Niu *et al.* fabricated a biomimetic nerve scaffold with a structure mimicking the native epineurium layer using PLLA nanofibers doped with gelatin[149]. In the sciatic nerve defect model of SD rats, the scaffold showed the effect of promoting the myelination of Schwann cells and the remolding of epineurium in the injured area, which could effectively rehabilitate the motor and sensory functions of the injured nerve and prevent the atrophy of the target muscle tissue. However, mechanical agitations on piezoelectric materials in most experiments relied on transient and random motions that were usually weak. The use of external mechanical sources, such as ultrasonic (US) generators, to transmit high-frequency mechanical waves with high spatial accuracy to target locations *in vivo* can provide more controllable and sustained mechanical stress to induce the conversion of mechanical stimuli into electrical charges of piezoelectric materials[151]. US stimulation can greatly enhance the generation of surface charge and associated electric field of piezoelectric materials enabling the interaction with surrounding cells and tissues[8,129,152,153], which could stimulate intracellular calcium activity, upregulate pertinent effector proteins, and promote tissue regeneration. It would be interesting to investigate the therapeutic efficacy of combining ultrasound and biodegradable piezoelectric materials. In addition, non-degradable components were often involved to achieve high piezoelectricity, and thus the development of piezoelectric nerve scaffolds ensuring complete biodegradation also needs further studies[154].

Moreover, biodegradable piezoelectric materials can also be applied to facilitate wound healing. Cutaneous wound healing mainly depends on transepithelial potentials, which could be modulated by the charges generated by piezoelectric materials[118]. Previous investigations revealed that electrical fields promoted wound healing through three stages [Figure 8E]. Firstly, in the inflammatory phase, electric fields enhanced blood flow and tissue oxygen to inhibit bacterial growth and reduce wound edema. Later in the proliferative phase, wound contraction, the proliferation of keratinocytes and fibroblasts, and the deposition of angiogenesis and collagen were accelerated. Collagen maturation and remodeling were subsequently promoted by electric fields in the remodeling phase[155]. Skin scaffolds or dermal patches fabricated by biodegradable piezoelectric materials have often resulted in accelerated wound healing. Park *et al*. showed that silk fibroin scaffolds facilitated the proliferative and remodeling phase of the wound healing process, through the canonical nuclear factor kappa enhancer binding protein (NF-κB) signaling pathway via the regulation of the expression of cyclin D1, vimentin, fibronectin, and vascular endothelial growth factor (VEGF)[156]. Based on polydopamine-coated chitosan films (CM@DA), Chen *et al*. reported a piezoelectric and photo-thermal film with a stable output voltage as mice were exercising [Figure 8F], and demonstrated desirable efficacy in promoting wound healing of mouse skin [Figure 8G][157]. Compared to pure chitosan films, CM@DA produced greater and more stable piezoelectric voltage following the movement of the rats. Combining CM@DA with near-infrared (NIR) light, the generated electric voltages and heat directly stimulated the expressions of heat shock protein 90 (Hsp90) and hypoxia-inducible factor 1α (HIF-1α). The elevated HIF-1α induced more Hsp90 secretion for cell migration, and the increase of Hsp90 effectively protected HIF-1α from degradation. The high expression level of HIF-1α can upregulate the expression of VEGF, which enhanced the formation of new blood vessels to assist the formation of granulation tissue and collagen deposition.

CONCLUSION

Given excellent biocompatibility, desirable biodegradability and tunable piezoelectric properties, biodegradable piezoelectric materials are attracting great attention for potential use in bioelectronics. We summarize the piezoelectric properties of representative organic biodegradable piezoelectric materials including small molecules such as amino acids and dipeptides and organic molecules with high order structure such as proteins, synthetic polymers and polysaccharides. Strategies to enhance piezoelectric activity are reviewed and applications for energy harvesting, actuators, sensors, transducers, and therapeutic devices are discussed.

To achieve commercial translation, a deeper understanding of the mechanism and characteristics of piezoelectricity of different biodegradable piezoelectric materials and appropriate engineering designs to adapt to specific medical scenarios are critical. Although with great progress, further advances are essential to overcome the existing challenges of organic biodegradable piezoelectric materials. Firstly, the longitudinal piezoelectric constants of these materials are generally much lower than the shear piezoelectric constants, which requires more complex structural design or processing schemes to compensate for the shortcomings. In addition, it remains a difficult task to simultaneously satisfy high piezoelectricity and desirable flexibility to adapt to the soft nature of biological tissues, as crystallinity contributes greatly to promoting piezoelectric activity that also comes along with mechanical stiffness. Moreover, rapid degradation of organic materials constrains the operational window, and appropriate biodegradable packaging materials are necessary to prolong the lifetime for extended application as implantable platforms. Materials strategies and fabrication schemes are essential to address these challenges, including the exploration of innovative biodegradable piezoelectric materials, new manufacturing methods to enhance the piezoelectric properties of existing materials, and the development of composite materials to balance piezoelectricity and flexibility. The incorporation of materials computation tools could also facilitate the

design of novel biodegradable piezoelectric materials and optimize relevant characteristics. In addition, the investigation of piezoelectrets offers an alternative pathway to realized biodegradable piezoelectric devices with fewer constraints in materials. Piezoelectrets can effectively act as piezoelectric materials by injecting charges or dipoles into a flexible material, which can greatly extend material options. Strategies to maintain the metastable injected charges remain the key to achieving practical utilization of piezoelectrets. Moreover, the exploitation of flexoelectric effects represents another interesting route to accomplish biodegradable electroactive devices beyond piezoelectric materials. In non-piezoelectric materials, the applied strain gradients could disrupt the previously highly symmetric charge density and result in polarization[158]. Although the flexoelectric effect is weak in most cases, flexible organic dielectric materials may have strong electrical responses under large strain gradients due to their low elastic modulus[159]. Some works have shown that flexoelectric effect could be used in energy harvesting[43,160-162], sensors and actuators[163].

In all, further developments will enable the optimization of biodegradable organic piezoelectric materials, which will open new avenues to achieve innovative bioelectronics such as energy devices, sensors, transducers and electronic medicine that can be fully resorbable, eliminating potential infection risks, and could play critical roles in healthcare.

DECLARATIONS

Authors' contributions

Did the literature review, outlined the manuscript structure, and wrote the manuscript draft: Dai F, Geng Q, Hua T, Yin L

Participated in the discussion of the review content: Sheng X, Yin L

Initiated the reviewing idea and were involved in the discussion and revision of the manuscript: Dai F, Yin L

All authors have read the manuscript and approved the final version.

Availability of data and materials

Not applicable.

Financial support and sponsorship

The authors acknowledge the support of the National Natural Science Foundation of China (52171239 and T2122010 to Yin L), Beijing Municipal Natural Science Foundation (Z220015 to Yin L), and Tsinghua University-Peking Union Medical College Hospital Initiative Scientific Research Program (20191080592).

Conflicts of interest

All authors declared that there are no conflicts of interest.

Ethical approval and consent to participate

Not applicable.

Consent for publication

Not applicable.

REFERENCES

1. Chorsi MT, Curry EJ, Chorsi HT, et al. Piezoelectric biomaterials for sensors and actuators. *Adv Mater* 2019;31:e1802084. DOI PubMed

2. Li J, Long Y, Yang F, Wang X. Degradable piezoelectric biomaterials for wearable and implantable bioelectronics. *Curr Opin Solid State Mater Sci* 2020;24:100806. DOI PubMed PMC
3. Dagdeviren C, Hwang SW, Su Y, et al. Transient, biocompatible electronics and energy harvesters based on ZnO. *Small* 2013;9:3398-404. DOI PubMed
4. Cung K, Han BJ, Nguyen TD, et al. Biotemplated synthesis of PZT nanowires. *Nano Lett* 2013;13:6197-202. DOI PubMed
5. Rödel J, Webber KG, Dittmer R, Jo W, Kimura M, Damjanovic D. Transferring lead-free piezoelectric ceramics into application. *J Eur Ceram Soc* 2015;35:1659-81. DOI
6. Jeong CK, Kim I, Park KI, et al. Virus-directed design of a flexible $BaTiO_3$ nanogenerator. *ACS Nano* 2013;7:11016-25. DOI PubMed
7. Okada K, Yanagisawa T, Kameshima Y, Nakajima A. Properties of TiO_2 prepared by acid treatment of $BaTiO_3$. *Mater Res Bull* 2007;42:1921-9. DOI
8. Zhu P, Chen Y, Shi J. Piezocatalytic tumor therapy by ultrasound-triggered and $BaTiO_3$-mediated piezoelectricity. *Adv Mater* 2020;32:e2001976. DOI PubMed
9. Wang Y, Zhou XY, Chen Z, et al. Synthesis of cubic $LiNbO_3$ nanoparticles and their application in vitro bioimaging. *Appl Phys A* 2014;117:2121-6. DOI
10. Yu S, Kuo S, Tuan W, Tsai Y, Wang S. Cytotoxicity and degradation behavior of potassium sodium niobate piezoelectric ceramics. *Ceram Int* 2012;38:2845-50. DOI
11. Liu F, Hashim NA, Liu Y, Abed MM, Li K. Progress in the production and modification of PVDF membranes. *J Membr Sci* 2011;375:1-27. DOI
12. Bystrov VS, Paramonova EV, Bdikin IK, Bystrova AV, Pullar RC, Kholkin AL. Molecular modeling of the piezoelectric effect in the ferroelectric polymer poly(vinylidene fluoride) (PVDF). *J Mol Model* 2013;19:3591-602. DOI PubMed
13. Beringer LT, Xu X, Shih W, Shih W, Habas R, Schauer CL. An electrospun PVDF-TrFe fiber sensor platform for biological applications. *Sens Actuators A Phys* 2015;222:293-300. DOI
14. Middleton JC, Tipton AJ. Synthetic biodegradable polymers as orthopedic devices. *Biomaterials* 2000;21:2335-46. DOI PubMed
15. Feig VR, Tran H, Bao Z. Biodegradable polymeric materials in degradable electronic devices. *ACS Cent Sci* 2018;4:337-48. DOI PubMed PMC
16. Tan MJ, Owh C, Chee PL, Kyaw AKK, Kai D, Loh XJ. Biodegradable electronics: cornerstone for sustainable electronics and transient applications. *J Mater Chem C* 2016;4:5531-58. DOI
17. Lemanov VV. Piezoelectric and pyroelectric properties of protein amino acids as basic materials of soft state physics. *Ferroelectrics* 2000;238:775-82. DOI
18. Lemanov VV, Popov SN, Pankova GA. Piezoelectric properties of crystals of some protein aminoacids and their related compounds. *Phys Solid State* 2002;44:1929-35. DOI
19. Perlovich GL, Hansen LK, Bauer-brandl A. The polymorphism of glycine - thermochemical and structural aspects. *J Therm Anal Calorim* 2001;66:699-715. DOI
20. Hu P, Hu S, Huang Y, et al. Bioferroelectric properties of glycine crystals. *J Phys Chem Lett* 2019;10:1319-24. DOI PubMed
21. Guerin S, Stapleton A, Chovan D, et al. Control of piezoelectricity in amino acids by supramolecular packing. *Nat Mater* 2018;17:180-6. DOI PubMed
22. Hamilton BD, Hillmyer MA, Ward MD. Glycine polymorphism in nanoscale crystallization chambers. *Cryst Growth Des* 2008;8:3368-75. DOI
23. Bishara H, Berger S. Polymorphism and piezoelectricity of glycine nano-crystals grown inside alumina nano-pores. *J Mater Sci* 2019;54:4619-25. DOI
24. Isakov D, Gomes EDM, Bdikin I, et al. Production of polar β-glycine nanofibers with enhanced nonlinear optical and piezoelectric properties. *Cryst Growth Des* 2011;11:4288-91. DOI
25. Hosseini ES, Manjakkal L, Shakthivel D, Dahiya R. Glycine-chitosan-based flexible biodegradable piezoelectric pressure sensor. *ACS Appl Mater Interfaces* 2020;12:9008-16. DOI PubMed PMC
26. Yang F, Li J, Long Y, et al. Wafer-scale heterostructured piezoelectric bio-organic thin films. *Science* 2021;373:337-42. DOI PubMed PMC
27. Guerin S, O'Donnell J, Haq EU, et al. Racemic amino acid piezoelectric transducer. *Phys Rev Lett* 2019;122:047701. DOI PubMed
28. Shrout TR, Zhang SJ. Lead-free piezoelectric ceramics: alternatives for PZT? *J Electroceram* 2007;19:113-26. DOI
29. Reches M, Gazit E. Casting metal nanowires within discrete self-assembled peptide nanotubes. *Science* 2003;300:625-7. DOI PubMed
30. Yan X, Zhu P, Li J. Self-assembly and application of diphenylalanine-based nanostructures. *Chem Soc Rev* 2010;39:1877-90. DOI PubMed
31. Kholkin A, Amdursky N, Bdikin I, Gazit E, Rosenman G. Strong piezoelectricity in bioinspired peptide nanotubes. *ACS Nano* 2010;4:610-4. DOI PubMed
32. Amdursky N, Beker P, Schklovsky J, Gazit E, Rosenman G. Ferroelectric and related phenomena in biological and bioinspired nanostructures. *Ferroelectrics* 2010;399:107-17. DOI
33. Vasilev S, Zelenovskiy P, Vasileva D, Nuraeva A, Shur VY, Kholkin AL. Piezoelectric properties of diphenylalanine microtubes prepared from the solution. *J Phys Chem Solids* 2016;93:68-72. DOI

34. Tao Z, Yuan H, Ding S, Wang Y, Hu W, Yang R. Diphenylalanine-based degradable piezoelectric nanogenerators enabled by polylactic acid polymer-assisted transfer. *Nano Energy* 2021;88:106229. DOI
35. Anderson J, Lake PT, McCullagh M. Initial aggregation and ordering mechanism of diphenylalanine from microsecond all-atom molecular dynamics simulations. *J Phys Chem B* 2018;122:12331-41. DOI PubMed
36. Nguyen V, Jenkins K, Yang R. Epitaxial growth of vertically aligned piezoelectric diphenylalanine peptide microrods with uniform polarization. *Nano Energy* 2015;17:323-9. DOI
37. Nguyen V, Zhu R, Jenkins K, Yang R. Self-assembly of diphenylalanine peptide with controlled polarization for power generation. *Nat Commun* 2016;7:13566. DOI PubMed PMC
38. Maziati Akmal MH, Ahmad FB, Hisham F, Hazmi AT. Advanced technology for the conversion of waste into fuels and chemicals. In: Khan A, Pizzi A, Jawaid M, et al., editors. 16-Biopolymer-based waste for biomaterials thin film in piezoelectric application. Woodhead Publishing; 2021. pp. 355-81. DOI
39. Bera S, Guerin S, Yuan H, et al. Molecular engineering of piezoelectricity in collagen-mimicking peptide assemblies. *Nat Commun* 2021;12:2634. DOI PubMed PMC
40. Yucel T, Cebe P, Kaplan DL. Structural origins of silk piezoelectricity. *Adv Funct Mater* 2011;21:779-85. DOI PubMed PMC
41. Zhou Z, Qian D, Minary-Jolandan M. Molecular Mechanism of polarization and piezoelectric effect in super-twisted collagen. *ACS Biomater Sci Eng* 2016;2:929-36. DOI PubMed
42. Ghosh SK, Mandal D. High-performance bio-piezoelectric nanogenerator made with fish scale. *Appl Phys Lett* 2016;109:103701. DOI
43. Yan Y, Kim W, Ma X, et al. Nanogenerators facilitated piezoelectric and flexoelectric characterizations for bioinspired energy harvesting materials. *Nano Energy* 2021;81:105607. DOI
44. Liu Y, Cai HL, Zelisko M, et al. Ferroelectric switching of elastin. *Proc Natl Acad Sci USA* 2014;111:E2780-6. DOI PubMed PMC
45. Wang R, Sui J, Wang X. Natural piezoelectric biomaterials: a biocompatible and sustainable building block for biomedical devices. *ACS Nano* 2022;16:17708-28. DOI PubMed
46. Stapleton A, Noor MR, Sweeney J, et al. The direct piezoelectric effect in the globular protein lysozyme. *Appl Phys Lett* 2017;111:142902. DOI
47. Karan SK, Maiti S, Kwon O, et al. Nature driven spider silk as high energy conversion efficient bio-piezoelectric nanogenerator. *Nano Energy* 2018;49:655-66. DOI
48. Kim D, Han SA, Kim JH, Lee JH, Kim SW, Lee SW. Biomolecular piezoelectric materials: from amino acids to living tissues. *Adv Mater* 2020;32:e1906989. DOI PubMed
49. Ghosh SK, Park J, Na S, Kim MP, Ko H. A fully biodegradable ferroelectric skin sensor from edible porcine skin gelatine. *Adv Sci* 2021;8:2005010. DOI PubMed PMC
50. Smith GP, Petrenko VA. Phage display. *Chem Rev* 1997;97:391-410. DOI PubMed
51. Dogic Z, Fraden S. Smectic phase in a colloidal suspension of semiflexible virus particles. *Phys Rev Lett* 1997;78:2417-20. DOI
52. Lee BY, Zhang J, Zueger C, et al. Virus-based piezoelectric energy generation. *Nat Nanotechnol* 2012;7:351-6. DOI PubMed
53. Shin D, Han HJ, Kim W, et al. Bioinspired piezoelectric nanogenerators based on vertically aligned phage nanopillars. *Energy Environ Sci* 2015;8:3198-203. DOI
54. Lee JH, Lee JH, Xiao J, Desai MS, Zhang X, Lee SW. Vertical self-assembly of polarized phage nanostructure for energy harvesting. *Nano Lett* 2019;19:2661-7. DOI PubMed
55. Park IW, Kim KW, Hong Y, et al. Recent developments and prospects of M13-bacteriophage based piezoelectric energy harvesting devices. *Nanomaterials* 2020;10:93. DOI PubMed PMC
56. Zhang J, Duan Y, Sato H, et al. Crystal modifications and thermal behavior of poly(l-lactic acid) revealed by infrared spectroscopy. *Macromolecules* 2005;38:8012-21. DOI
57. Wang H, Zhang J, Tashiro K. Phase transition mechanism of poly(l-lactic acid) among the α, δ, and β forms on the basis of the reinvestigated crystal structure of the β form. *Macromolecules* 2017;50:3285-300. DOI
58. Shin DM, Hong SW, Hwang YH. Recent advances in organic piezoelectric biomaterials for energy and biomedical applications. *Nanomaterials* 2020;10:123. DOI PubMed PMC
59. Shao J, Sun J, Bian X, et al. Modified PLA homochiral crystallites facilitated by the confinement of PLA stereocomplexes. *Macromolecules* 2013;46:6963-71. DOI
60. Cartier L, Okihara T, Ikada Y, Tsuji H, Puiggali J, Lotz B. Epitaxial crystallization and crystalline polymorphism of polylactides. *Polymer* 2000;41:8909-19. DOI
61. Ochiai T, Fukada E. Electromechanical properties of poly-L-lactic acid. *Jpn J Appl Phys* 1998;37:3374. DOI
62. Babichuk IS, Lin C, Qiu Y, et al. Raman mapping of piezoelectric poly(l-lactic acid) films for force sensors. *RSC Adv* 2022;12:27687-97. DOI PubMed PMC
63. Mat Zin S, Velayutham T, Furukawa T, et al. Quantitative study on the face shear piezoelectricity and its relaxation in uniaxially-drawn and annealed poly-l-lactic acid. *Polymer* 2022;254:125095. DOI
64. Lovell CS, Fitz-gerald JM, Park C. Decoupling the effects of crystallinity and orientation on the shear piezoelectricity of polylactic acid. *J Polym Sci B Polym Phys* 2011;49:1555-62. DOI
65. Tajitsu Y. Development of environmentally friendly piezoelectric polymer film actuator having multilayer structure. *Jpn J Appl Phys* 2016;55:04EA07. DOI

66. Mossi KM, Selby GV, Bryant RG. Thin-layer composite unimorph ferroelectric driver and sensor properties. *Mater Lett* 1998;35:39-49. DOI
67. Curry EJ, Ke K, Chorsi MT, et al. Biodegradable piezoelectric force sensor. *Proc Natl Acad Sci USA* 2018;115:909-14. DOI PubMed PMC
68. Nalwa HS. Ferroelectric polymers: chemistry: physics, and applications. Nalwa HS: Boca Raton; 1995. DOI
69. Lee SJ, Arun AP, Kim KJ. Piezoelectric properties of electrospun poly(l-lactic acid) nanofiber web. *Mater Lett* 2015;148:58-62. DOI
70. Zhao G, Huang B, Zhang J, Wang A, Ren K, Wang ZL. Electrospun poly(l-lactic acid) nanofibers for nanogenerator and diagnostic sensor applications. *Macromol Mater Eng* 2017;302:1600476. DOI
71. Sultana A, Ghosh SK, Sencadas V, et al. Human skin interactive self-powered wearable piezoelectric bio-e-skin by electrospun poly-l-lactic acid nanofibers for non-invasive physiological signal monitoring. *J Mater Chem B* 2017;5:7352-9. DOI PubMed
72. Curry EJ, Le TT, Das R, et al. Biodegradable nanofiber-based piezoelectric transducer. *Proc Natl Acad Sci USA* 2020;117:214-20. DOI PubMed PMC
73. Imoto K, Date M, Fukada E, et al. Piezoelectric motion of poly(l-lactic acid) film improved by supercritical CO_2 treatment. *Jpn J Appl Phys* 2009;48:09KE06. DOI
74. Sawano M, Tahara K, Orita Y, Nakayama M, Tajitsu Y. New design of actuator using shear piezoelectricity of a chiral polymer, and prototype device: actuator using shear piezoelectricity of a chiral polymer. *Polym Int* 2010;59:365-70. DOI
75. Fukada E. History and recent progress in piezoelectric polymers. *IEEE Trans Ultrason Ferr* 2000;47:1277-90. DOI PubMed
76. Ribeiro C, Sencadas V, Correia DM, Lanceros-Méndez S. Piezoelectric polymers as biomaterials for tissue engineering applications. *Colloids Surf B* 2015;136:46-55. DOI PubMed
77. Fukada E, Ando Y. Piezoelectric properties of poly-β-hydroxybutyrate and copolymers of β-hydroxybutyrate and β-hydroxyvalerate. *Int J Biol Macromol* 1986;8:361-6. DOI
78. Chernozem R, Guselnikova O, Surmeneva M, et al. Diazonium chemistry surface treatment of piezoelectric polyhydroxybutyrate scaffolds for enhanced osteoblastic cell growth. *Appl Mater Today* 2020;20:100758. DOI
79. Urakami T, Imagawa S, Harada M, Iwamoto A, Tokiwa Y. Development of biodegradable plastic-poly-β-hydroxybutyrate/polycaprolactone blend polymer. *Kobunshi Ronbunshu* 2000;57:263-70. DOI
80. García Y, Ruiz-Blanco YB, Marrero-Ponce Y, Sotomayor-Torres CM. Orthotropic piezoelectricity in 2D nanocellulose. *Sci Rep* 2016;6:34616. DOI PubMed PMC
81. Moon RJ, Martini A, Nairn J, Simonsen J, Youngblood J. Cellulose nanomaterials review: structure, properties and nanocomposites. *Chem Soc Rev* 2011;40:3941-94. DOI PubMed
82. Csoka L, Hoeger IC, Rojas OJ, Peszlen I, Pawlak JJ, Peralta PN. Piezoelectric effect of cellulose nanocrystals thin films. *ACS Macro Lett* 2012;1:867-70. DOI PubMed
83. Maiti S, Kumar Karan S, Lee J, Kumar Mishra A, Bhusan Khatua B, Kon Kim J. Bio-waste onion skin as an innovative nature-driven piezoelectric material with high energy conversion efficiency. *Nano Energy* 2017;42:282-93. DOI
84. Rajala S, Siponkoski T, Sarlin E, et al. Cellulose nanofibril film as a piezoelectric sensor material. *ACS Appl Mater Interfaces* 2016;8:15607-14. DOI PubMed
85. Sierra DL, Bdikin I, Tkach A, Vilarinho PM, Nunes C, Ferreira P. Flexible piezoelectric chitosan and barium titanate biocomposite films for sensor applications. *Eur J Inorg Chem* 2021;2021:792-803. DOI
86. de Marzo G, Mastronardi VM, Algieri L, et al. Sustainable, flexible, and biocompatible enhanced piezoelectric chitosan thin film for compliant piezosensors for human health. *Adv Electron Mater* 2022:2200069. DOI
87. Jacob J, More N, Kalia K, Kapusetti G. Piezoelectric smart biomaterials for bone and cartilage tissue engineering. *Inflamm Regen* 2018;38:2. DOI PubMed PMC
88. Hoque NA, Thakur P, Biswas P, et al. Biowaste crab shell-extracted chitin nanofiber-based superior piezoelectric nanogenerator. *J Mater Chem A* 2018;6:13848-58. DOI
89. Zhukov S, Ma X, Seggern HV, et al. Biodegradable cellular polylactic acid ferroelectrets with strong longitudinal and transverse piezoelectricity. *Appl Phys Lett* 2020;117:112901. DOI
90. Gao X, Huang L, Wang B, et al. Natural materials assembled, biodegradable, and transparent paper-based electret nanogenerator. *ACS Appl Mater Interfaces* 2016;8:35587-92. DOI PubMed
91. Mohebbi A, Mighri F, Ajji A, Rodrigue D. Cellular polymer ferroelectret: a review on their development and their piezoelectric properties. *Adv Polym Technol* 2018;37:468-83. DOI
92. Ouassim H, Frej M, Denis R. Piezoelectric cellular polymer films: fabrication, properties and applications. *AIMS Mater Sci* 2018;5:845-69. DOI
93. Felig P. Amino acid metabolism in man. *Annu Rev Biochem* 1975;44:933-55. DOI PubMed
94. Tóthová L, Bábíčková J, Celec P. Phage survival: the biodegradability of M13 phage display library in vitro. *Biotechnol Appl Biochem* 2012;59:490-4. DOI PubMed
95. Merzlyak A, Indrakanti S, Lee SW. Genetically engineered nanofiber-like viruses for tissue regenerating materials. *Nano Lett* 2009;9:846-52. DOI PubMed
96. Hajitou A, Trepel M, Lilley CE, et al. A hybrid vector for ligand-directed tumor targeting and molecular imaging. *Cell* 2006;125:385-98. DOI PubMed
97. Walton M, Cotton NJ. Long-term in vivo degradation of poly-L-lactide (PLLA) in bone. *J Biomater Appl* 2007;21:395-411. DOI

PubMed

98. Bos RR, Rozema FR, Boering G, et al. Degradation of and tissue reaction to biodegradable poly(L-lactide) for use as internal fixation of fractures: a study in rats. *Biomaterials* 1991;12:32-6. DOI PubMed
99. Bergsma JE, de Bruijn WC, Rozema FR, Bos RR, Boering G. Late degradation tissue response to poly(L-lactide) bone plates and screws. *Biomaterials* 1995;16:25-31. DOI PubMed
100. Beguin P. The biological degradation of cellulose. *FEMS Microbiol Rev* 1994;13:25-58. DOI
101. Helenius G, Bäckdahl H, Bodin A, Nannmark U, Gatenholm P, Risberg B. In vivo biocompatibility of bacterial cellulose. *J Biomed Mater Res A* 2006;76:431-8. DOI PubMed
102. Zhou H, Zhang Y, Qiu Y, et al. Stretchable piezoelectric energy harvesters and self-powered sensors for wearable and implantable devices. *Biosens Bioelectron* 2020;168:112569. DOI PubMed
103. Marino A, Genchi GG, Sinibaldi E, Ciofani G. Piezoelectric effects of materials on bio-interfaces. *ACS Appl Mater Interfaces* 2017;9:17663-80. DOI PubMed
104. Jenkins K, Kelly S, Nguyen V, Wu Y, Yang R. Piezoelectric diphenylalanine peptide for greatly improved flexible nanogenerators. *Nano Energy* 2018;51:317-23. DOI
105. Lee JH, Heo K, Schulz-Schönhagen K, et al. Diphenylalanine peptide nanotube energy harvesters. *ACS Nano* 2018;12:8138-44. DOI PubMed
106. Zhao C, Zhang J, Wang ZL, Ren K. A poly(l-lactic acid) polymer-based thermally stable cantilever for vibration energy harvesting applications. *Adv Sustain Syst* 2017;1:1700068. DOI
107. Hu D, Yao M, Fan Y, Ma C, Fan M, Liu M. Strategies to achieve high performance piezoelectric nanogenerators. *Nano Energy* 2019;55:288-304. DOI
108. Wu C, Wang AC, Ding W, Guo H, Wang ZL. Triboelectric nanogenerator: a foundation of the energy for the new era. *Adv Energy Mater* 2019;9:1802906. DOI
109. Xu Q, Gao X, Zhao S, et al. Construction of bio-piezoelectric platforms: from structures and synthesis to applications. *Adv Mater* 2021;33:e2008452. DOI PubMed
110. Olvera D, Monaghan MG. Electroactive material-based biosensors for detection and drug delivery. *Adv Drug Deliv Rev* 2021;170:396-424. DOI PubMed
111. Mahapatra SD, Mohapatra PC, Aria AI, et al. Piezoelectric materials for energy harvesting and sensing applications: roadmap for future smart materials. *Adv Sci* 2021;8:e2100864. DOI PubMed PMC
112. Tajitsu Y. Development of electric control catheter and tweezers for thrombosis sample in blood vessels using piezoelectric polymeric fibers. *Polym Adv Technol* 2006;17:907-13. DOI
113. Liu J, Li W, Jia J, et al. Structure-regenerated silk fibroin with boosted piezoelectricity for disposable and biodegradable oral healthcare device. *Nano Energy* 2022;103:107787. DOI
114. Kim K, Ha M, Choi B, et al. Biodegradable, electro-active chitin nanofiber films for flexible piezoelectric transducers. *Nano Energy* 2018;48:275-83. DOI
115. Ben Dali O, Zhukov S, Rutsch M, et al. Biodegradable 3D-printed ferroelectret ultrasonic transducer with large output pressure. *IEEE Int Ultra Sym* 2021:1-4. DOI
116. Whited JL, Levin M. Bioelectrical controls of morphogenesis: from ancient mechanisms of cell coordination to biomedical opportunities. *Curr Opin Genet Dev* 2019;57:61-9. DOI PubMed PMC
117. Goonoo N, Bhaw-luximon A. Piezoelectric polymeric scaffold materials as biomechanical cellular stimuli to enhance tissue regeneration. *Mater Today Commun* 2022;31:103491. DOI
118. Kapat K, Shubhra QTH, Zhou M, Leeuwenburgh S. Piezoelectric nano-biomaterials for biomedicine and tissue regeneration. *Adv Funct Mater* 2020;30:1909045. DOI
119. Khare D, Basu B, Dubey AK. Electrical stimulation and piezoelectric biomaterials for bone tissue engineering applications. *Biomaterials* 2020;258:120280. DOI PubMed
120. Shimono T, Matsunaga S, Fukada E, Hattori T, Shikinami Y. The effects of piezoelectric poly-L-lactic acid films in promoting ossification in vivo. *In Vivo* 1996;10:471-6. PubMed
121. Chen Y, Mak AF, Wang M, Li J, Wong M. PLLA scaffolds with biomimetic apatite coating and biomimetic apatite/collagen composite coating to enhance osteoblast-like cells attachment and activity. *Surf Coat Technol* 2006;201:575-80. DOI
122. Prabhakaran MP, Venugopal J, Ramakrishna S. Electrospun nanostructured scaffolds for bone tissue engineering. *Acta Biomater* 2009;5:2884-93. DOI PubMed
123. Kramp B, Bernd HE, Schumacher WA, et al. [Poly-beta-hydroxybutyric acid (PHB) films and plates in defect covering of the osseus skull in a rabbit model]. *Laryngorhinootologie* 2002;81:351-6. DOI PubMed
124. Wang YW, Wu Q, Chen GQ. Attachment, proliferation and differentiation of osteoblasts on random biopolyester poly(3-hydroxybutyrate-co-3-hydroxyhexanoate) scaffolds. *Biomaterials* 2004;25:669-75. DOI PubMed
125. Ye C, Hu P, Ma MX, Xiang Y, Liu RG, Shang XW. PHB/PHBHHx scaffolds and human adipose-derived stem cells for cartilage tissue engineering. *Biomaterials* 2009;30:4401-6. DOI PubMed
126. Rocha LB, Goissis G, Rossi MA. Biocompatibility of anionic collagen matrix as scaffold for bone healing. *Biomaterials* 2002;23:449-56. DOI PubMed
127. Moreira PL, An YH, Santos AR Jr, Genari SC. In vitro analysis of anionic collagen scaffolds for bone repair. *J Biomed Mater Res B*

Appl Biomater 2004;71:229-37. DOI PubMed
128. Amaral IF, Cordeiro AL, Sampaio P, Barbosa MA. Attachment, spreading and short-term proliferation of human osteoblastic cells cultured on chitosan films with different degrees of acetylation. *J Biomater Sci Polym Ed* 2007;18:469-85. DOI PubMed
129. Das R, Curry EJ, Le TT, et al. Biodegradable nanofiber bone-tissue scaffold as remotely-controlled and self-powering electrical stimulator. *Nano Energy* 2020;76:105028. DOI
130. Liu Y, Dzidotor G, Le TT, et al. Exercise-induced piezoelectric stimulation for cartilage regeneration in rabbits. *Sci Transl Med* 2022;14:eabi7282. DOI PubMed
131. Liu L, Chen B, Liu K, et al. Wireless manipulation of magnetic/piezoelectric micromotors for precise neural stem-like cell stimulation. *Adv Funct Mater* 2020;30:1910108. DOI
132. Zhao D, Feng PJ, Liu JH, et al. Electromagnetized-nanoparticle-modulated neural plasticity and recovery of degenerative dopaminergic neurons in the mid-brain. *Adv Mater* 2020;32:e2003800. DOI PubMed
133. Du L, Li T, Jin F, et al. Design of high conductive and piezoelectric poly(3,4-ethylenedioxythiophene)/chitosan nanofibers for enhancing cellular electrical stimulation. *J Colloid Interface Sci* 2020;559:65-75. DOI PubMed
134. Zuo KJ, Gordon T, Chan KM, Borschel GH. Electrical stimulation to enhance peripheral nerve regeneration: update in molecular investigations and clinical translation. *Exp Neurol* 2020;332:113397. DOI PubMed
135. Huang J, Ye Z, Hu X, Lu L, Luo Z. Electrical stimulation induces calcium-dependent release of NGF from cultured Schwann cells. *Glia* 2010;58:622-31. DOI PubMed
136. Wu P, Chen P, Xu C, et al. Ultrasound-driven in vivo electrical stimulation based on biodegradable piezoelectric nanogenerators for enhancing and monitoring the nerve tissue repair. *Nano Energy* 2022;102:107707. DOI
137. Chen P, Xu C, Wu P, et al. Wirelessly powered electrical-stimulation based on biodegradable 3D piezoelectric scaffolds promotes the spinal cord injury repair. *ACS Nano* 2022;16:16513-28. DOI PubMed
138. Yang F, Murugan R, Ramakrishna S, Wang X, Ma YX, Wang S. Fabrication of nano-structured porous PLLA scaffold intended for nerve tissue engineering. *Biomaterials* 2004;25:1891-900. DOI PubMed
139. Yang F, Murugan R, Wang S, Ramakrishna S. Electrospinning of nano/micro scale poly(L-lactic acid) aligned fibers and their potential in neural tissue engineering. *Biomaterials* 2005;26:2603-10. DOI PubMed
140. Chen W, Tong YW. PHBV microspheres as neural tissue engineering scaffold support neuronal cell growth and axon-dendrite polarization. *Acta Biomater* 2012;8:540-8. DOI PubMed
141. Naseri-Nosar M, Salehi M, Hojjati-Emami S. Cellulose acetate/poly lactic acid coaxial wet-electrospun scaffold containing citalopram-loaded gelatin nanocarriers for neural tissue engineering applications. *Int J Biol Macromol* 2017;103:701-8. DOI PubMed
142. Rinaudo M. Chitin and chitosan: properties and applications. *Prog Polym Sci* 2006;31:603-32. DOI
143. Kuo YC, Yeh CF, Yang JT. Differentiation of bone marrow stromal cells in poly(lactide-co-glycolide)/chitosan scaffolds. *Biomaterials* 2009;30:6604-13. DOI PubMed
144. Wang S, Sun C, Guan S, et al. Chitosan/gelatin porous scaffolds assembled with conductive poly(3,4-ethylenedioxythiophene) nanoparticles for neural tissue engineering. *J Mater Chem B* 2017;5:4774-88. DOI PubMed
145. Eltom A, Zhong G, Muhammad A. Scaffold techniques and designs in tissue engineering functions and purposes: a review. *Adv Mater Sci Eng* 2019;2019:1-13. DOI
146. Ceballos D, Navarro X, Dubey N, Wendelschafer-Crabb G, Kennedy WR, Tranquillo RT. Magnetically aligned collagen gel filling a collagen nerve guide improves peripheral nerve regeneration. *Exp Neurol* 1999;158:290-300. DOI PubMed
147. Bian YZ, Wang Y, Aibaidoula G, Chen GQ, Wu Q. Evaluation of poly(3-hydroxybutyrate-co-3-hydroxyhexanoate) conduits for peripheral nerve regeneration. *Biomaterials* 2009;30:217-25. DOI PubMed
148. Yucel D, Kose GT, Hasirci V. Polyester based nerve guidance conduit design. *Biomaterials* 2010;31:1596-603. DOI PubMed
149. Niu Y, Stadler FJ, Fu M. Biomimetic electrospun tubular PLLA/gelatin nanofiber scaffold promoting regeneration of sciatic nerve transection in SD rat. *Mater Sci Eng C Mater Biol Appl* 2021;121:111858. DOI PubMed
150. Jiang Z, Song Y, Qiao J, et al. Rat sciatic nerve regeneration across a 10-mm defect bridged by a chitin/CM-chitosan artificial nerve graft. *Int J Biol Macromol* 2019;129:997-1005. DOI PubMed
151. Cafarelli A, Marino A, Vannozzi L, et al. Piezoelectric nanomaterials activated by ultrasound: the pathway from discovery to future clinical adoption. *ACS Nano* 2021;15:11066-86. DOI PubMed PMC
152. Genchi GG, Ceseracciu L, Marino A, et al. P(VDF-TrFE)/$BaTiO_3$ nanoparticle composite films mediate piezoelectric stimulation and promote differentiation of SH-SY5Y neuroblastoma cells. *Adv Healthc Mater* 2016;5:1808-20. DOI PubMed
153. Hoop M, Chen XZ, Ferrari A, et al. Ultrasound-mediated piezoelectric differentiation of neuron-like PC12 cells on PVDF membranes. *Sci Rep* 2017;7:4028. DOI PubMed PMC
154. Zaszczynska A, Sajkiewicz P, Gradys A. Piezoelectric scaffolds as smart materials for neural tissue engineering. *Polymers* 2020;12:161. DOI
155. Ashrafi M, Alonso-Rasgado T, Baguneid M, Bayat A. The efficacy of electrical stimulation in experimentally induced cutaneous wounds in animals. *Vet Dermatol* 2016;27:235-e257. DOI PubMed
156. Park YR, Sultan MT, Park HJ, et al. NF-κB signaling is key in the wound healing processes of silk fibroin. *Acta Biomater* 2018;67:183-95. DOI
157. Chen Y, Ye M, Song L, et al. Piezoelectric and photothermal dual functional film for enhanced dermal wound regeneration via

upregulation of Hsp90 and HIF-1α. *Appl Mater Today* 2020;20:100756. DOI

158. Deng Q, Liu L, Sharma P. Flexoelectricity in soft materials and biological membranes. *J Mech Phys Solids* 2014;62:209-27. DOI
159. Grasinger M, Mozaffari K, Sharma P. Flexoelectricity in soft elastomers and the molecular mechanisms underpinning the design and emergence of giant flexoelectricity. *Proc Natl Acad Sci USA* 2021:118. DOI PubMed PMC
160. Wang B, Yang S, Sharma P. Flexoelectricity as a universal mechanism for energy harvesting from crumpling of thin sheets. *Phys Rev B* 2019:100. DOI
161. Rahmati AH, Yang S, Bauer S, Sharma P. Nonlinear bending deformation of soft electrets and prospects for engineering flexoelectricity and transverse d(31) piezoelectricity. *Soft Matter* 2018;15:127-48. DOI
162. Jiang X, Huang W, Zhang S. Flexoelectric nano-generator: materials, structures and devices. *Nano Energy* 2013;2:1079-92. DOI
163. Abdollahi A, Arias I. Constructive and destructive interplay between piezoelectricity and flexoelectricity in flexural sensors and actuators. *J Appl Mech* 2015;82:121003. DOI